Contract No.
DE-AS05-78ER0604

DOE/ER/06042--8

DE88 004520

# PROPERTIES OF LANTHANIDE OXIDES AS SUPPORTS FOR TRANSITION METAL CATALYSTS

Progress Report for the Period

May 1, 1987 to April 30, 1988

by

Michael P. Rosynek

Department of Chemistry
Texas A & M University
College Station, Texas 77843





Submitted:
December, 1987

## OBJECTIVES

The objective of this research program has been to provide an understanding of the manner in which variations in metal precursors and oxidic support materials, particularly lanthanide oxides, influence the reduction behaviors and catalytic/surface properties of dispersed non-noble Group VIII transition metals. Support materials selected for study provide appropriate variations in several important physical/chemical properties, including acid-base character and cationic multi-valency. The goals of the project have been to attain an increased understanding of the general phenomenon of support effects, and to enable correlations to be made between physical/chemical properties of support materials and the catalytic behaviors of transition metals that are dispersed on their surfaces. Our research effort during the past year has comprised two principal areas of investigation involving support/precursor effects, viz., hydrocarbon conversion and surface carbon formation on dispersed nickel catalysts, and reduction behaviors/catalytic properties of supported cobalt. Details of research progress in these two areas are provided in the following sections.

## SUMMARY OF RESEARCH PROGRESS

### Hydrocarbon Conversion on Supported Nickel

Reactions of n-alkanes over supported nickel catalysts at ~400°C result in the formation of hydrogen-deficient carbonaceous species (i.e., coke) on the catalyst surface. It is not certain whether the deposited coke remains localized on the metallic sites that led to its formation or migrates onto the support material. The gaseous hydrogen that is released during this process subsequently reacts with additional alkane to form hydrogenolysis/-hydrocracking products, as well as with the deposited carbonaceous surface species to produce both aromatic homologation products and (possibly) additional $C_1$ - $C_5$ non-aromatic products. In the case of n-hexane reactant,

for example, the overall process can be represented by the following generalized reaction scheme:

$$n\text{-}C_6H_{14} \xrightarrow{\sim 400^\circ C} CH_x\,(s) + H_2\,(g) \qquad (1)$$

$$n\text{-}C_6H_{14} + H_2 \longrightarrow C_1 - C_5 \text{ Alkanes} \qquad (2)$$

$$CH_x + H_2 \rightleftharpoons \begin{matrix} \text{Aromatics} \\ C_1 - C_5 \text{ Alkanes} \end{matrix} \qquad (3)$$

The principal emphasis of our study of this system has been to investigate the effects of variations in support, metal loading level, reaction temperature, and n-alkane reactant in influencing the selectivity of the above conversion processes.

Catalysts. The nickel catalysts used for this study were prepared by impregnation of the various supports to incipient wetness, using aqueous solutions of $Ni(NO_3)_2$, followed by vacuum drying at 110°C. Three catalysts, having loading levels of 0.5, 2.0, and 5.0 wt% Ni (reduced basis) were prepared for each of three supports having a wide range of surface areas. All catalysts were reduced prior to use by treatment in flowing $H_2$ for 16 h at 400°C. Properties of the nine catalysts used are summarized in Table 1.

Table 1

Properties of Supported Nickel Catalysts

| Support | S.A. ($m^2/g$) | — % Metal Reduction — 0.5% | 2.0% | 5.0% | Metal Exposure (H/Ni) 0.5% | 2.0% | 5.0% |
|---|---|---|---|---|---|---|---|
| $La_2O_3$ | 15 | 73 | 100 | 95 | 0.11 | 0.14 | 0.14 |
| $SiO_2$ Gel | 290 | 35 | 58 | 63 | 0.67 | 0.46 | 0.35 |
| Charcoal | 1200 | 6 | 10 | 16 | 1.11 | 1.02 | 0.95 |

Extents of metal reduction were determined (assuming NiO formation) by pulse titration with $O_2$ at 450°C, except for the charcoal-supported catalysts, which were done at 200°C, using the system described in the next paragraph; metal exposures were measured by $H_2$ adsorption at 0°C.

Procedure. All reaction studies were performed using a grease-free, stainless steel pulse-flow system with a tubular quartz reactor containing a 50 mg catalyst sample. Pulses of n-hexane or n-butane reactant (each containing ~10% as many moles of hydrocarbon reactant as total moles of reduced, exposed Ni in the catalyst sample) were injected into a helium stream that flowed continuously through the reactor. After passing through the catalyst bed, each pulse of products plus unconverted reactant was carried directly into the inlet of a gas chromatograph, where separation and analysis of the pulse occurred. The amount of uneluted carbonaceous surface species deposited during each pulse was calculated by a difference method. Total amounts of surface carbon, as determined by quantitative combustion in $O_2$ after each experiment, typically agreed within ~10% with the cumulative calculated amounts.

Results and Discussion. Results for a typical pulse experiment, using n-hexane reactant at 400°C over a 5 wt% $Ni/SiO_2$ catalyst are shown in Fig. 1, which displays certain features that were commonly observed. Total conversion of successive reactant pulses decreases with increasing deposition of surface carbon, although the extent of conversion decline is markedly influenced by reaction temperature and catalyst identity (see below). The fraction of each pulse that reacts to form surface carbon remains almost constant for at least the first 20 pulses, corresponding to a total amount of deposited carbon equivalent to several monolayers. Initial pulses of hydrocarbon reactant are converted primarily into carbonaceous surface species, with the concomitantly released hydrogen reacting with additional hydrocarbon to produce primarily non-aromatic $C_1$ - $C_5$ paraffins. Aromatic products begin to appear only

after several previous pulses have deposited adequate surface carbonaceous species to react with gaseous $H_2$. Significantly, although ~80% of the total aromatic products formed during n-hexane reaction is benzene, toluene and naphthalene are also observed. It is not yet clear whether reaction of surface carbon also leads to non-aromatic products (the lower branch of reaction (3) above) simultaneously with formation of aromatics. In most experiments, relatively little change in the distribution of gaseous products was observed after about the fifth pulse in a series, and all data in subsequent Figures are shown for pulse No. 5

We have investigated the effects of variations in reaction temperature, support material, and hydrocarbon reactant on the reaction selectivity for each metal loading level. Results for n-hexane conversion over $Ni/SiO_2$ at three reaction temperatures in the range 325 to 475°C are summarized in Figs. 2-4. At each temperature, total conversion generally increases and aromatics formation decreases with increases metal loading level. Hence, formation of surface carbon that reacts with gaseous $H_2$ to produce aromatic products appears to be increasingly favored on smaller metal particles (see table above). It is also clear from these data that, for a given support and metal loading, increasing reaction temperature causes a decrease in selectivity to aromatic products, but has relatively little effect on that of surface carbon formation.

The influence of variations in support material and, indirectly, metal particle size (as shown by differing metal exposures) is illustrated in Figs. 5-7 for reaction of n-hexane at 400°C. Use of the low surface area $La_2O_3$ support (Fig. 5), on which Ni particles are extensively reduced but relatively large, results initially in complete conversion of each pulse, but leads to almost exclusive formation of surface carbonaceous species, with virtually no evolution of gaseous products. With the $SiO_2$ support, on the other hand (Fig. 6), only ~60% of the fifth pulse is converted to surface carbon on each catalyst. On this support, aromatic products decrease and non-aromatics increase with increasing metal particle size (increasing loading level). The

greatest selectivity to aromatics occurred with the charcoal-supported catalysts (Fig. 7), although the variation with metal loading level is not as smooth as for the $La_2O_3$ and $SiO_2$ supports.

The nature of the surface carbon reaction leading to aromatic product formation was investigated by employing n-butane reactant. Results for three $Ni/SiO_2$ catalysts at a reaction temperature of 400°C are shown in Fig. 8. Although the extent of aromatics formation is somewhat less for each of the three catalysts than those observed using n-hexane reactant under identical conditions (Fig. 3), results for the two reactant are, in general, similar. It is significant that aromatic products are observed during reaction of n-butane, since, unlike the case for n-hexane reactant, unimolecular formation of an aromatic ring is not possible. The generation of benzene from n-butane has the same significance as the formation of toluene and higher aromatics from n-hexane. The carbonaceous surface species that is deposited during reaction of any saturated hydrocarbon may have a pseudo-aromatic or ring-like structure that tends to react with gaseous $H_2$ to produce principally aromatic species. We plan to perform a series of tracer experiments involving pulses of isotopically-labelled n-$^{13}C_6H_{14}$ and n-$^{13}C_4H_{10}$ reactants, in an attempt to elucidate the genesis of gaseous aromatic products during these hydrocarbon conversion reactions.

The results of this investigation of supported nickel catalysts can be summarized by the following conclusions:

1.) Selectivity of n-alkane conversion over dispersed nickel catalysts is markedly influenced by variations in support material, metal loading, and reaction temperature.

2.) For n-hexane reactant, selectivity to aromatic products increases with:

   a.) Decreasing metal loading level and, hence, increasing metal exposure and decreasing metal particle size.

   b.) Decreasing reaction temperature.

3.) Selectivity to carbonaceous surface species during n-alkane conversion increases with increasing metal particle size, but is relatively unaffected by variations in reaction temperature.

**Reduction and Catalytic Properties of Supported Cobalt**

The second principal area of emphasis in this project has been an investigation of the effects of variations in support and metal precursor on the reduction behaviors of dispersed cobalt catalysts and on their corresponding activity/selectivity characteristics for CO hydrogenation. A series of catalysts containing ~6 wt% Co was prepared by an incipient wetness impregnation technique, using aqueous solutions of $Co(NO_3)_2$, $CoCl_2$, and $Co(CH_3COO)_2$; supports employed included a fumed silica (Cab-O-Sil), $La_2O_3$, and $CeO_2$. Pre-calcination, when performed, was in $O_2$ for 16 h at 500°C; reduction treatments involved exposure to circulating $H_2$ for 8 h at either 400 or 700°C. All CO hydrogenation experiments were carried out in a recirculation, batch-type reactor at a reaction temperature of 250°C and an initial $H_2/CO$ reactant ratio of 2/1 at 1 atm total pressure.

The effects of variations in support, metal precursor, calcination, and reduction temperature on catalyst behaviors for CO hydrogenation are summarized in Table 2. Certain generalizations can be made on the basis of these data.

**Effect of Support.** Among the catalyst and treatment variables investigated, support identity has the most pronounced and predictable effect on selectivity for the CO hydrogenation reaction over dispersed cobalt. For each of the three metal precursors, both the average hydrocarbon product chain length and the $C_2 + C_3$ olefin/paraffin ratio increases in the following order, regardless of reduction temperature, calcination, or overall catalyst activity:

$$Co/SiO_2 < Co/CeO_2 < Co/La_2O_3$$

Table 2

Results for CO Hydrogenation over Supported Cobalt Catalysts[1]

| Support | Precursor | Calcination | Reduction Temp(°C) | Initial Activity[2] | Ave. HC Length[3] | O/P Ratio[4] |
|---|---|---|---|---|---|---|
| $SiO_2$ | $Co(NO_3)_2$ | No | 400 | 26.0 | 1.3 | 0.3 |
| | | No | 700 | 40.4 | 1.3 | 0.2 |
| | | Yes | 400 | 5.2 | 1.3 | 0.3 |
| | | Yes | 700 | 9.0 | 1.7 | 1.9 |
| | $CoCl_2$ | No | 400 | 0.05 | 1.3 | 0.2 |
| | | No | 700 | < 0.01 | - | - |
| | | Yes | 400 | 9.5 | 1.2 | 0.4 |
| | | Yes | 700 | 1.3 | 1.2 | 0.4 |
| | $Co(CH_3COO)_2$ | No | 400 | 3.0 | 1.3 | 0.2 |
| | | No | 700 | 12.0 | 1.2 | 0.4 |
| | | Yes | 400 | 18.1 | 1.4 | 0.4 |
| | | Yes | 700 | 0.6 | 1.5 | 0.9 |
| $CeO_2$ | $Co(NO_3)_2$ | No | 400 | 10.1 | 1.8 | 1.7 |
| | | No | 700 | 0.5 | 1.6 | 0.4 |
| | | Yes | 400 | 6.6 | 1.9 | 1.8 |
| | | Yes | 700 | 0.1 | 1.6 | 0.9 |
| | $CoCl_2$ | No | 400 | 0.09 | - | - |
| | | No | 700 | 0.03 | - | - |
| | | Yes | 400 | 0.01 | - | - |
| | | Yes | 700 | < 0.01 | - | - |
| | $Co(CH_3COO)_2$ | No | 400 | 0.01 | - | - |
| | | No | 700 | < 0.01 | - | - |
| | | Yes | 400 | 1.6 | 2.0 | 2.4 |
| | | Yes | 700 | 0.02 | - | - |
| $La_2O_3$ | $Co(NO_3)_2$ | No | 400 | 5.7 | 2.1 | 3.0 |
| | | No | 700 | 10.8 | 2.0 | 4.0 |
| | | Yes | 400 | < 0.01 | - | - |
| | | Yes | 700 | < 0.01 | - | - |
| | $CoCl_2$ | No | 400 | 36.4 | 2.2 | 2.9 |
| | | No | 700 | < 0.01 | - | - |
| | | Yes | 400 | < 0.01 | - | - |
| | | Yes | 700 | 0.05 | - | - |
| | $Co(CH_3COO)_2$ | No | 400 | 0.01 | - | - |
| | | No | 700 | 3.9 | 2.1 | 3.2 |
| | | Yes | 400 | < 0.01 | - | - |
| | | Yes | 700 | 13.1 | 1.8 | 2.8 |

[1] Reaction conditions: 250°C, 1 atm, $H_2/CO = 2/1$
[2] mole CO/mole Co-sec x $10^4$ at 5% CO conversion
[3] Accurate chain lengths and O/P ratios could not be calculated for activities < ~0.1
[4] For $C_2 + C_3$ hydrocarbons

Under the reaction conditions used in this study, the hydrocarbon product over $Co/SiO_2$ is > 75% methane (average chain length = ~1.3) and is largely paraffinic, indicating that extensive secondary hydrogenation of the primary olefin product occurs. In comparison, corresponding average chain lengths over $Co/CeO_2$ and $Co/La_2O_3$ are ~1.9 and 2.2, respectively.

In contrast to the observed pattern of selectivity behavior, trends in overall catalytic activity are more complex. Variations in metal precursor, pre-calcination, and, to a lesser extent, reduction temperature all play important roles in determining activity for CO hydrogenation over cobalt, and few generalizations can be made. Pre-calcination of all three precursors on the $La_2O_3$ support invariably results in very low catalytic activity when subsequent $H_2$ reduction is at 400°C, while much higher activity is attained when reduction is performed at 700°C. Powder x-ray diffraction (XRD) data indicate that each of the three cobalt salts undergoes a solid-state reaction with $La_2O_3$ during calcination to produce the perovskite $LaCoO_3$. The latter requires substantially higher temperatures for reduction in $H_2$ than is the case for the $Co_3O_4$ that is generated by calcination of $SiO_2$- and $CeO_2$-supported precursors. Both temperature-programmed reduction (TPR) and x-ray photoelectron spectroscopic (XPS) results confirm that reduction of all three cobalt precursors occurs much more readily on $CeO_2$ than on either $SiO_2$ or $La_2O_3$. It appears that the presence of the multi-valent cerium cations in $CeO_2$ plays an important role in promoting cobalt reduction.

Effect of Precursor. At both reduction temperatures, the nitrate precursor, in general, leads to the most active catalysts for CO hydrogenation. On both $SiO_2$ and $CeO_2$ supports, the chloride salt produces catalysts having activities more than two orders of magnitude lower than those derived from the nitrate. Although TPR profiles indicate that the chloride salt is easily reducible, the low activities of chloride-derived catalysts are probably due to poisoning of metallic sites by residual $Cl^-$ ions, whose presence on these materials following reduction treatment has been confirmed by

XPS. Significantly, the $CoCl_2/La_2O_3$ starting material results in a very active catalyst, despite the presence of residual $Cl^-$, due to anion scavenging by the highly basic $La_2O_3$ support.

The acetate precursor is more varied in its behavior on the three supports than are the other two cobalt salts. On $SiO_2$, it leads to catalysts having activities comparable to those of nitrate-derived catalysts, particularly after calcination, while on $CeO_2$ measurable activity is only achieved by $H_2$ reduction at 400°C of a pre-calcined material. With $La_2O_3$-supported acetate, activity for CO hydrogenation is negligible following $H_2$ treatment at 400°C of either a calcined or uncalcined starting material, but high activity is attained in both cases when a reduction temperature of 700°C is employed. TPR measurements indicate that, in addition to the expected formation of $CH_4$ and $CO_2$, thermal treatment of $Co(CH_3COO)_2/La_2O_3$ also results in evolution of substantial amounts of gaseous $H_2$. The latter is presumably derived from the highly labile surface hydroxyls on this support. This thermal process requires temperatures > 500°C for completion and may account for the lack of significant catalytic activity following $H_2$ treatment at only 400°C.

## PUBLICATIONS

A manuscript entitled "$NH_3$ and $CO_2$ Adsorption onto $La_2O_3$," based on results obtained in this investigation, has recently been submitted for publication in the Journal of Catalysis. A copy of this manuscript is enclosed for reference purposes.

## PERSONNEL

The following two graduate students, both doctoral candidates, are currently being supported by funding from this project:

Dale R. Palke

Christine A. Polansky

FIGURE 1

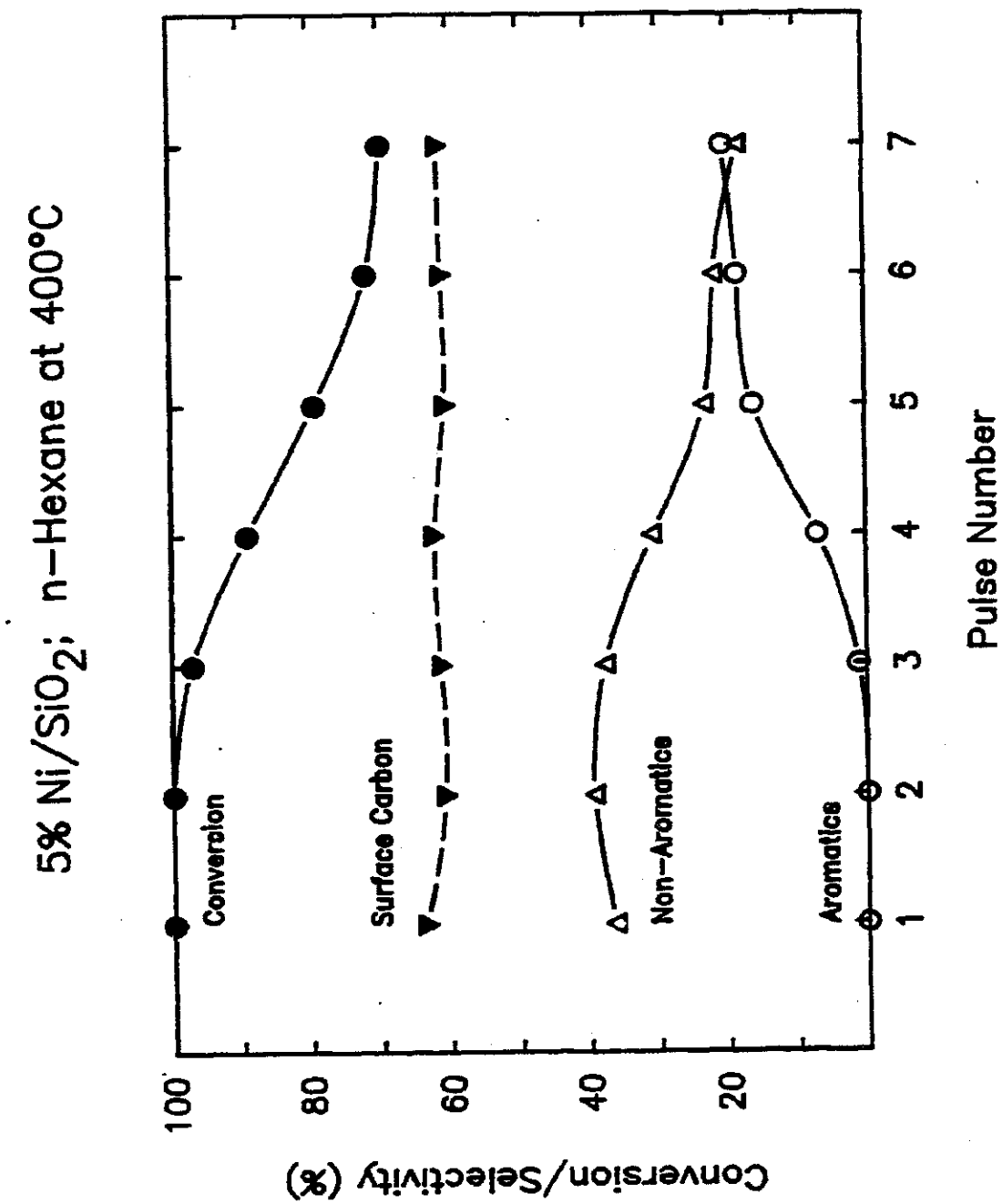
5% Ni/SiO2; n-Hexane at 400°C
Conversion/Selectivity (%)
100
80
60
40
20
Conversion
Surface Carbon
Non-Aromatics
Aromatics
1
2
3
4
5
6
7
Pulse Number

FIGURE 2

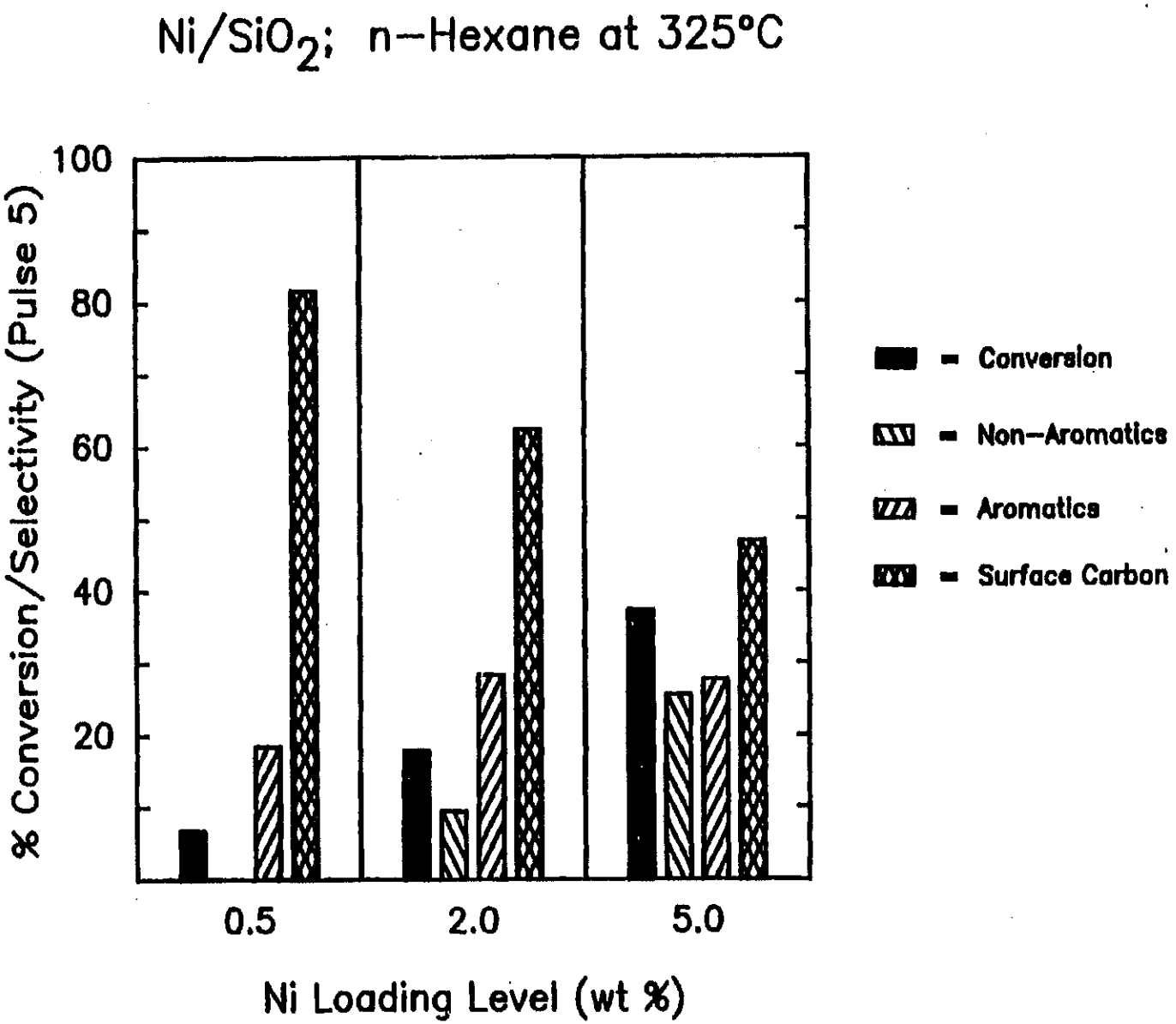
Ni/SiO2; n-Hexane at 325°C
% Conversion/Selectivity (Pulse 5)
100
80
60
40
20
0.5
2.0
5.0
Ni Loading Level (wt %)
= Conversion
= Non-Aromatics
= Aromatics
= Surface Carbon

FIGURE 3

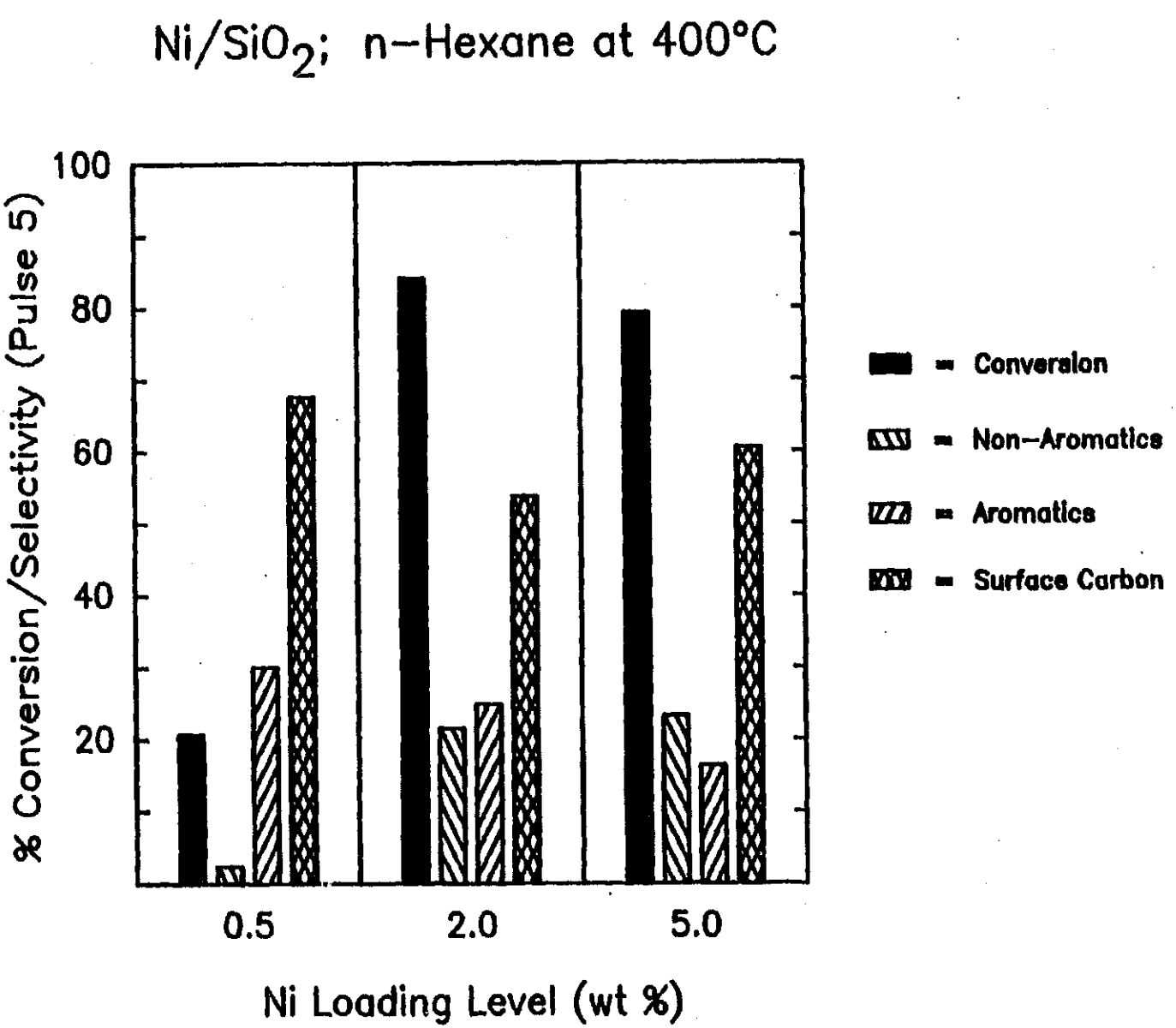
Ni/SiO2; n-Hexane at 400°C
% Conversion/Selectivity (Pulse 5)
100
80
60
40
20
0.5
2.0
5.0
Ni Loading Level (wt %)
= Conversion
= Non-Aromatics
= Aromatics
= Surface Carbon

FIGURE 4

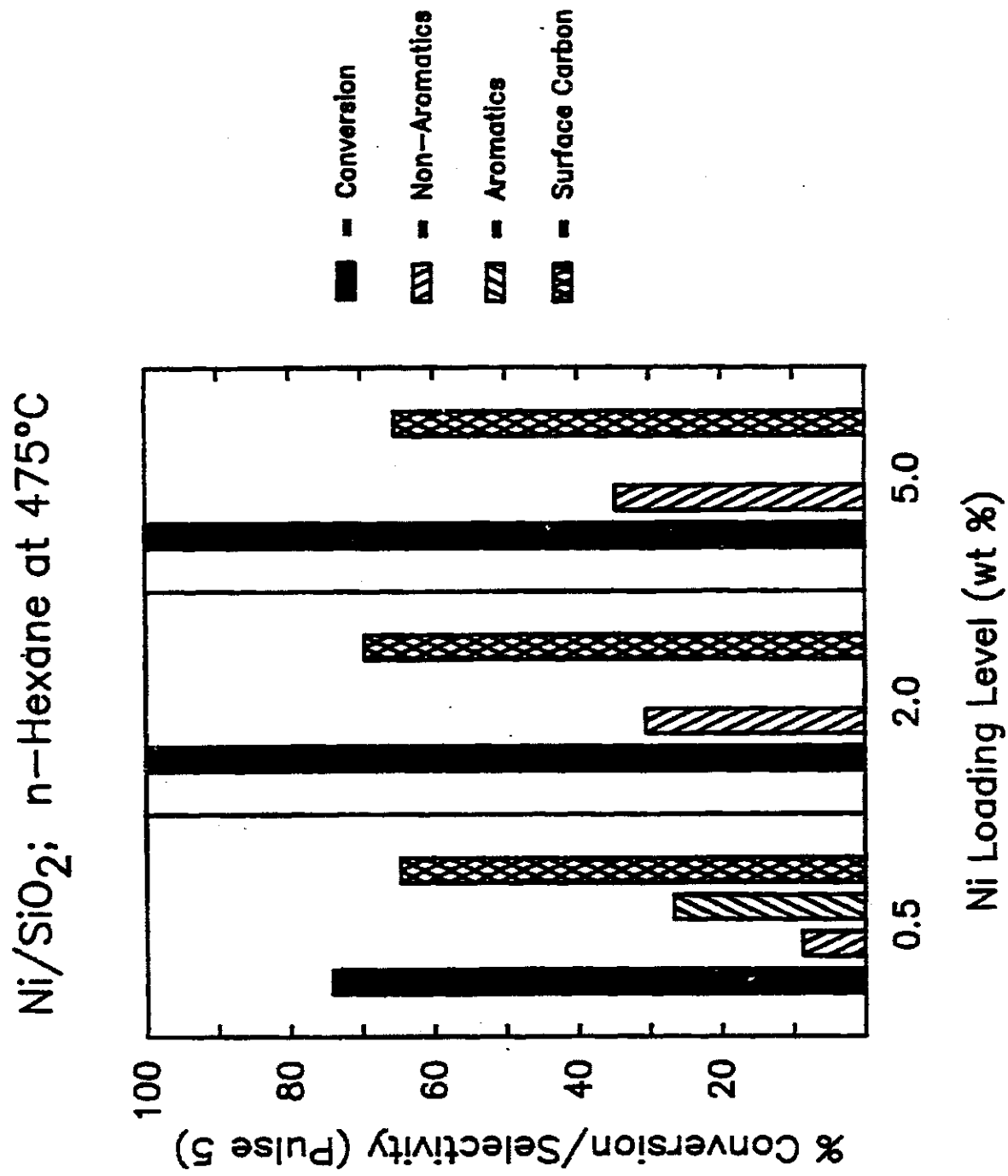
Ni/SiO2; n-Hexane at 475°C
Conversion
Non-Aromatics
Aromatics
Surface Carbon
% Conversion/Selectivity (Pulse 5)
100
80
60
40
20
0.5
2.0
5.0
Ni Loading Level (wt %)

FIGURE 5

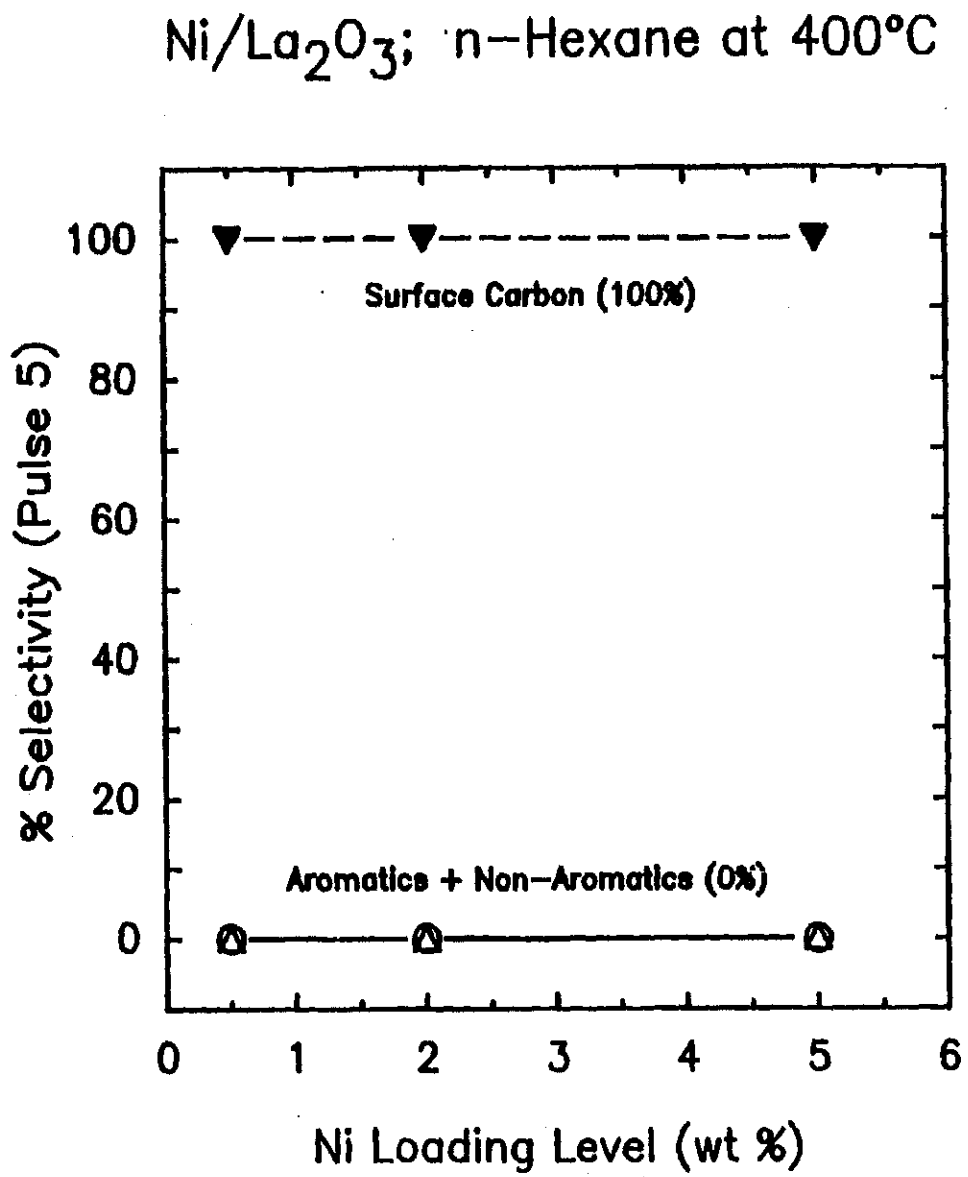
Ni/La2O3; n-Hexane at 400°C
100
80
60
40
20
0
% Selectivity (Pulse 5)
Surface Carbon (100%)
Aromatics + Non-Aromatics (0%)
0
1
2
3
4
5
6
Ni Loading Level (wt %)

FIGURE 6

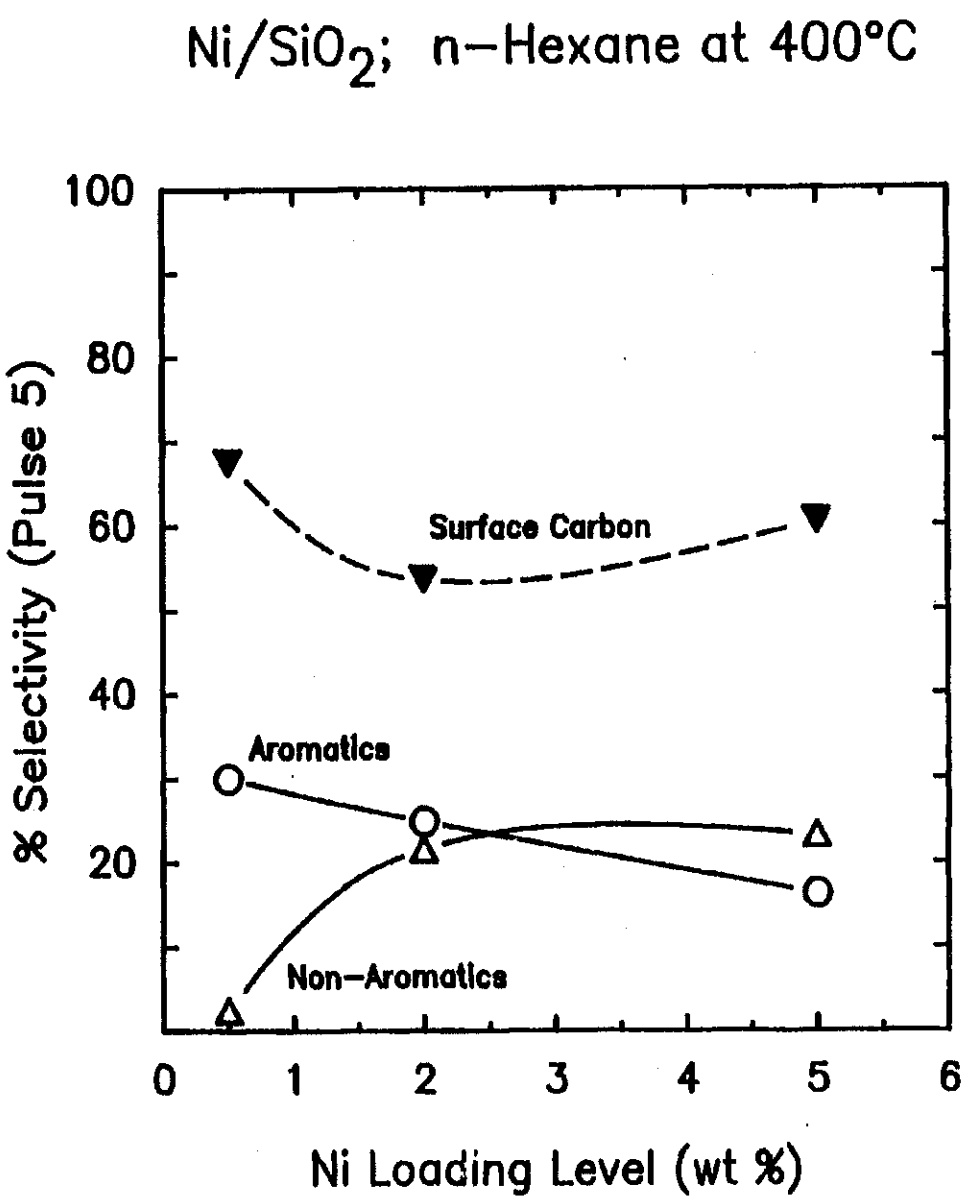
Ni/SiO2; n-Hexane at 400°C
% Selectivity (Pulse 5)
100
80
60
40
20
0
1
2
3
4
5
6
Surface Carbon
Aromatics
Non-Aromatics
Ni Loading Level (wt %)

FIGURE 7

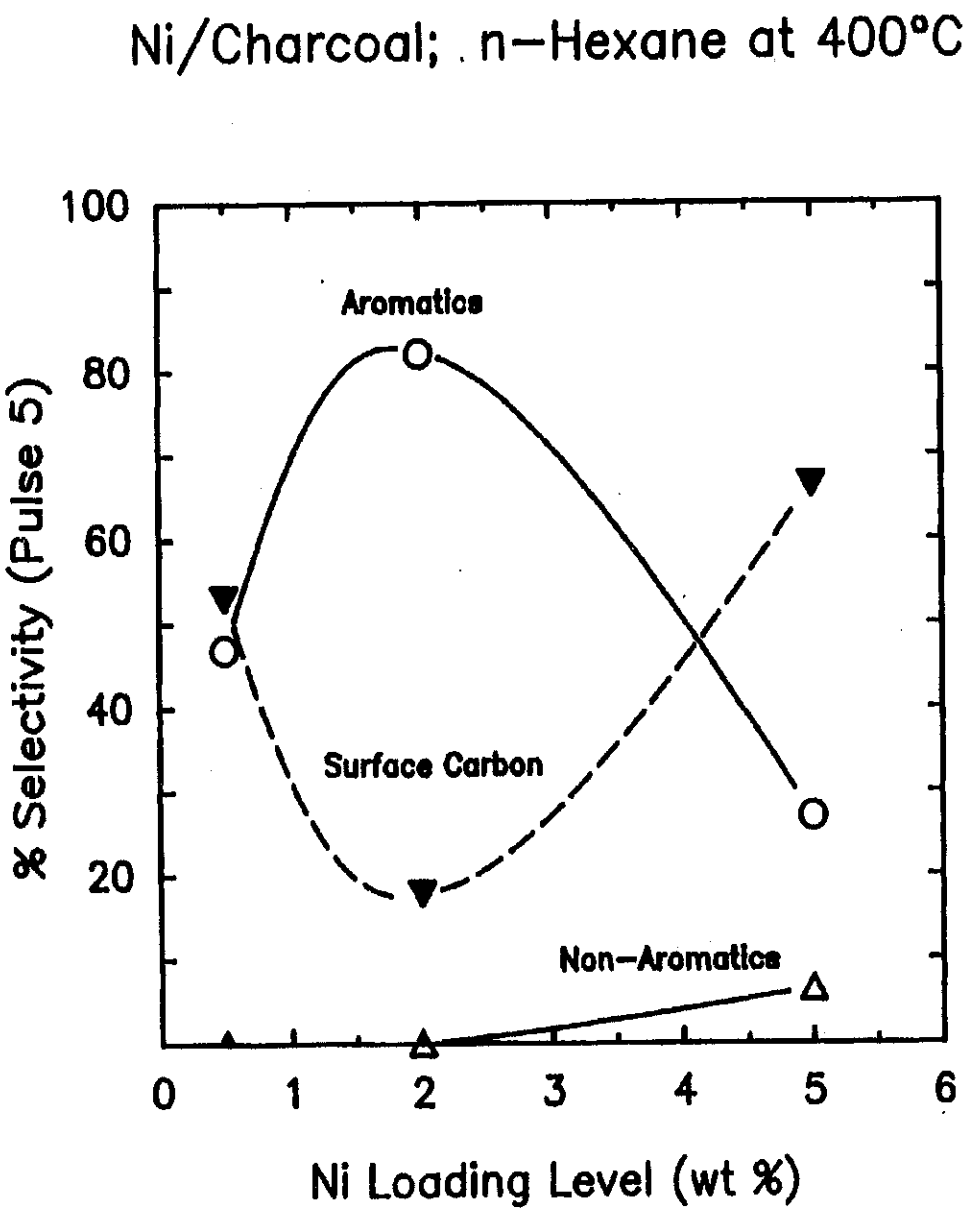
Ni/Charcoal; n-Hexane at 400°C
% Selectivity (Pulse 5)
100
80
60
40
20
0
1
2
3
4
5
6
Ni Loading Level (wt %)
Aromatics
Surface Carbon
Non-Aromatics

FIGURE 8

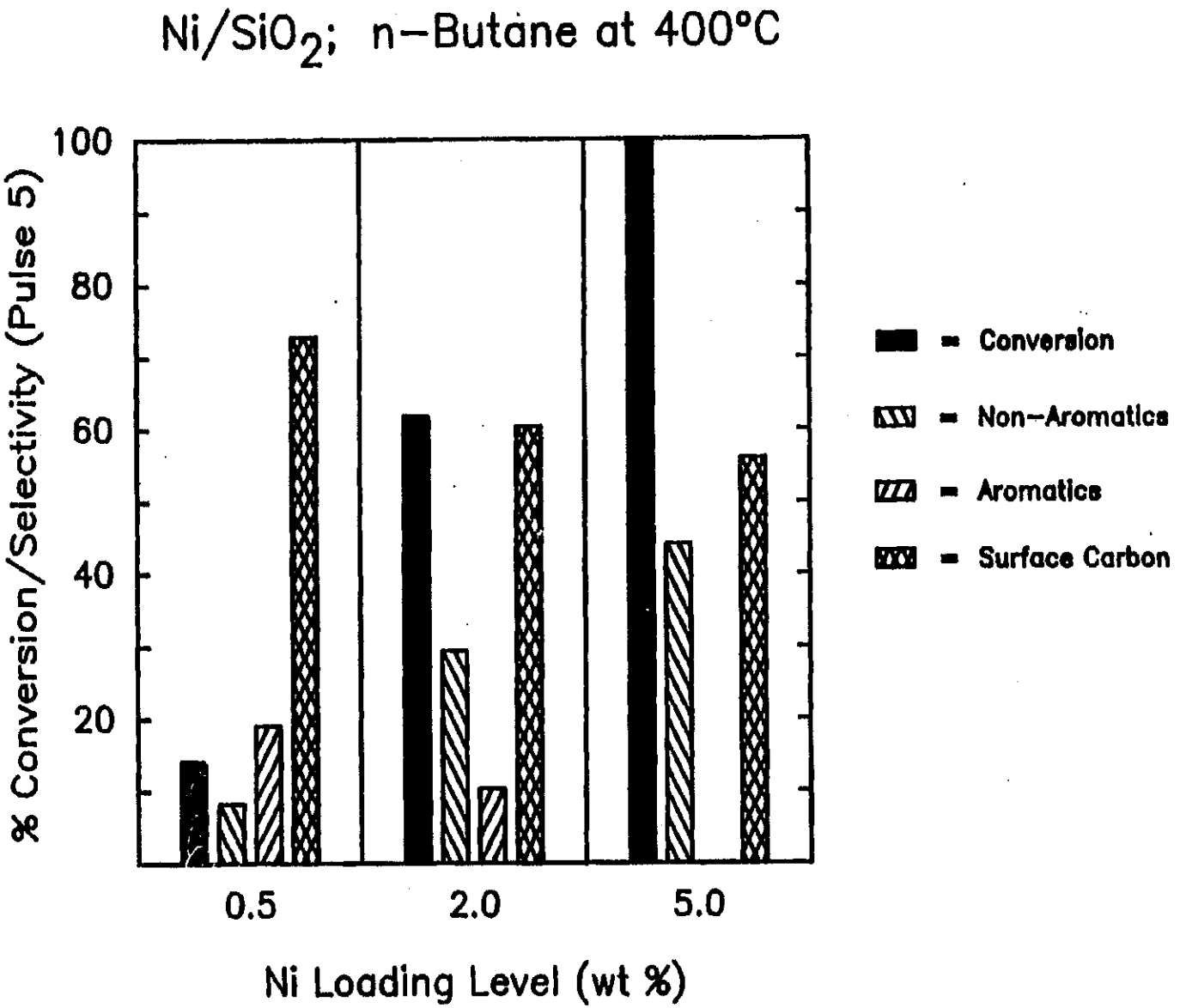
Ni/SiO2; n-Butane at 400°C
% Conversion/Selectivity (Pulse 5)
100
80
60
40
20
0.5
2.0
5.0
Ni Loading Level (wt %)
= Conversion
= Non-Aromatics
= Aromatics
= Surface Carbon

# $NH_3$ AND $CO_2$ ADSORPTION ONTO $La_2O_3$

by

Michael P. Rosynek[1] and Gregory N. DelliSante

Department of Chemistry, Texas A&M University
College Station, Texas 77843

Running Title: $NH_3$ and $CO_2$ Adsorption onto $La_2O_3$

## ABSTRACT

$NH_3$ and $CO_2$ adsorption onto an evacuated $La_2O_3$ surface was investigated. $NH_3$ adsorption at 50°C led to weak, nondissociative-coordination of $NH_3$ molecules to $La^{3+}$ sites via the nitrogen lone-pair electrons. However, with $CO_2$, bonding at 50°C was to surface $O^{-2}$ ions. Generated were unidentate carbonates which rearranged at 350°C to bidentate coordination. By reacting an $NH_3$ and $CO_2$ mixture on $La_2O_3$ at 50°C carbamate species were formed. At 250°C, these entities dehydrated to cyanate species coordinated to $La^{3+}$ sites through the oxygen atom. Above 500°C, the surface bonding rearranged to produce stronger, bidentate linkage, and above 800°C, polymerization produce were observed. $CO_2$ adsorption was shown to reverse the bidentate-linked cyanate back to the weaker, unidentate coordination. $H_2O$ exposure at 350°C reverses the entire dehydration by converting the cyanates back to $NH_3$ and $CO_2$. Mechanisms and adsorption sites for these reactions are discussed.

# INTRODUCTION

$La_2O_3$ displays a wide variety of catalytic behaviors some of which are unique to the lanthanide oxides. Despite this, few studies which reveal the nature of adsorption sites have been reported. Certain specific types of adsorption sites can often be shown to be catalytically active. These adsorption sites can be characterized by carefully analyzing the chemisorption of well-defined gaseous probe molecules. $NH_3$ and $CO_2$ have been shown to be poisons for a number of catalytic reactions which occur on $La_2O_3$. The weak and dissimilar acid-base properties of these molecules also makes them a good combination for probing surface sites. However, $NH_3$ and $CO_2$ adsorption on $La_2O_3$ has been largely ignored except for an investigation by Minachev et al. (1). They detected and analyzed one adsorbed specie for each adsorbate by thermal desorption, but were unable to determine the actual modes of adsorption. Additionally, no interaction between the chemisorbed species was detected. In the present study, transmission IR spectroscopy was used to more-definitively investigate the nature of these $NH_3$ and $CO_2$ adsorption sites on $La_2O_3$.

## EXPERIMENTAL METHODS

Materials. Ventron $La_2O_3$ was completely rehydrated in boiling water open to the atmosphere to obtain $La(OH)_3$ from which IR samples were made. The oxygen used came from Airco, Inc., and was high purity grade (99.9%). It was further purified by passage through a glass-bead-filled trap maintained at -196°C. Distilled $H_2O$ was further purified by numerous freeze-pump-thaw cycles at -78°C. Prior exposure to activated charcoal was required to completely remove organic impurities. Anhydrous grade $NH_3$ (99.9%) was obtained from Matheson Gas Products Co. $NH_3$ (98% atom % D) was obtained from Merck and Co., Inc. $^{15}NH_3$ (99 atom % N-15) was from Stohler Isotope Chemicals. All three ammonias were freeze-pumped at -78°C and -196°C. The $NH_3$ was additionally exposed to an excess of similarly pretreated $La_2O_3$ prior to sample exposure to remove last traces of impurities. Linde instrument grade $CO_2$ (99.9%) was used. $^{13}CO_2$ (99 atom % C-13) and $C^{18}O_2$ (99 atom % O-18) were both obtained from Stohler Isotope Chemicals. The carbon dioxides were each passed through a trap at -78°C before use. HCN was generated by mixing concentrated reagent grade $H_2SO_4$ and reagent grade KCN followed by drying over reagent grade, anhydrous $P_2O_5$.

Apparatus. For transmission IR studies a Vycor IR cell of standard design with KCl windows was employed. A furnace capable of quickly attaining 1000°C was wrapped around its shaft. A separate Vycor sample holder vertically suspended a chip of $La_2O_3$ sample on a thin copper wire which could be internally wound. This windless arrangement allowed delicate movement of the sample from the viewing to heating area with high precision. All work was done in an all-glass system equipped with a hot-oil diffusion pump in

series with a mechanical forepump capable of attaining pressures of $10^{-6}$ torr.

A Perkin-Elmer 399 repetitive scanning IR was mounted around the IR cell. The IR cell itself was clamped to the vacuum system for the life of each sample. These steps assured a reproducibility of at least 5 percent in the gas adsorption technique, which was required for quantitative measurements.

Procedure. In a typical experiment, $La(OH)_3$ was hand ground for about an hour and then weighed and pressed at 5000 p.s.i. between steel disks to obtain a 15 x 10 mm wafer of about 40 mg $La_2O_3/cm^2$ optical density. Once the wafer was placed in the IR cell, the cell itself would be clamped to the vacuum system, and the surface of the sample cleansed by 24 hours of vacuum heating at 800°C. This treatment included one hour of $O_2$ treatment at 800°C toward the end of this period. However such $O_2$ treatment would always be followed by at least 30 minutes of vacuum heating. A background spectrum would reveal a lack of adsorbed species and assure that A-type $La_2O_3$ has been formed to an adequate degree. This surface was either used in an experiment, or, alternatively, the sample was then re-exposed to about 22 torr of water in the vacuum system at 25°C for 3 hours so as to completely rehydrate the $La_2O_3$ back to $La(OH)_3$. Next, dehydration at 600-800°C for a short time would convert the material back to A-type $La_2O_3$. This more-timely pretreatment was sometimes done to increase the surface area of the starting oxide. The surface area of a sample thus treated was still typically only 7 $m^2/g$.

During an experiment, a background scan was taken and stored in computer memory. A probe gas was then admitted to the sample with the sample temperature maintained from 25-900°C. However all IR spectra themselves were

taken with the sample maintained at about 50°C (IR beam heating alone). Following removal of the probe gas at the exposure temperature, and sample cooling to ambient temperature, a spectrum would be taken with the new adsorbed species and the background spectrum subtracted from it before final display. Additionally, each individual spectrum was ensemble averaged numerous times by repetitive scanning. Only chemisorbed species at equilibrium (Relative to the scanning time) could be quantitatively studied by this procedure. By interpreting the bonding nature of the adsorbed probe molecules, information about the behavior of adsorption sites was obtained.

## RESULTS AND DISCUSSION

### $NH_3$ Adsorption

When $NH_3$ was exposed to $La_2O_3$ at 50°C the only resulting IR band was a single, fairly broad and symmetric, extremely weak band at 1092 $cm^{-1}$d. An illustration of this response appears in Figure 1. The band reached full intensity within minutes following exposure. With evacuation the band immediately shifted to 1132 $cm^{-1}$. This dependence of band position on adsorbate pressure is a common observation, and reflects additional $NH_3$ adsorption onto weaker sites as the $NH_3$ pressure was increased. All IR evidence of chemisorbed species vanished following vacuum heating at only 130°C for about 20 minutes. Removal of chemisorbed $NH_3$ by vacuum heating at about 250°C, followed by readsorption of $NH_3$ at about 50°C, resulted in the same quantity of adsorbed $NH_3$. Therefore, the $NH_3$ adsorption was both nondestructive and reproducible.

Deuterium and N-15 labeled $NH_3$ were also adsorbed. With $NH_3$ adsorption the bands each shifted about 200 $cm^{-1}$. Using $^{15}NH_3$, the bands each shifted 5-10 $cm^{-1}$. These shifts suggest the origin of the band as the symmetric deformation of an $NH_3$ molecule coordinated to a $La^{3+}$ site via the nitrogen lone-pair electrons. The symmetric deformation is well-known to produce the most intense band in the gas phase $NH_3$ spectrum and appears at 968 and 932 $cm^{-1}$. The band is split due to inversion doubling. For the gas phase $NH_3$ spectrum, isotopic labeling with $ND_3$ and $^{15}NH_3$ results in shifts of 202 and 6 $cm^{-1}$, respectively, and these correspond to the values observed for the $NH_3$ surface species (2).

For the general population of inorganic coordination compounds, three deformation vibrations of ligated $NH_3$ molecules occur. The degenerate

deformation is observed in the region of 1650-1560 $cm^{-1}$, the symmetric deformation in the region 1350-1150 $cm^{-1}$, and the $NH_3$ rocking frequency from 950-650 $cm^{-1}$ (3). This is consistent with the present assignment for $NH_3$ adsorption on $La_2O_3$.

IR studies of $NH_3$ adsorption on oxide surfaces have been reviewed (4,5,6). However, the rare earths as absorbents have been largely ignored. One reason may be that on basic oxides, acid sites are often believed to have a less significant effect on catalytic activity than the effect of basic sites. On the more acidic oxide $Al_2O_3$, Peri used $NH_3$ adsorption as probe to detect changes in the concentration of acid sites during pretretment (7). Results were strongly corrected to catalytic results. Since $Al_{23}$ derives its catalytic nature from its strongly acidic Lewis acid sites, this is not unexpected. An IR study of $NH_3$ adsorption onto a number of oxide surfaces has been reported by Filimonov et al. (8). They examined $NH_3$ adsorption onto a number of metal oxides. Their results are consistent with those obtained on $La_2O_3$. They observed a band due to the symmetric deformation of coordinated $NH_3$ molecules at 1280-1240, 1220, 1220, 1230-1190, 1180 and 1070-1110 $cm^{-1}$ for $Al_2O_3$, BeO, ZnO, $ZrO_2$, NiO, and MgO, respectively. A similar study was reported by Minachev et al. (1); however, thermal gravimetric desorption was used instead of IR spectroscopy to detect adsorbed $NH_3$ on both acidic and basic oxides. On the acidic $Al_2O_3$, three types of strongly adsorbed $NH_3$ were identified. Adsorption of $NH_3$ onto the basic oxides of La and Nd was also verified. Adsorption onto La and Nd oxides was the weakest, resulting in removal of all adsorbed species following vacuum heating at only 115°C, which is in agreement with the present results. Morimote et al. performed an IR study of $NH_3$ adsorption onto ZnO (9). Even the acid sites on

ZnO were strong enough to cause dissociative adsorption to produce surface amides. Although the acid sites on $La_2O_3$ appear much weaker, they probably exist in large number. $LaCl_3$ has been determined to coordinate large quantities of $NH_3$, with coordination numbers as great as nine (10). The acid sites on $La_2O_3$, compared to those on other oxides are therefore seen to be quite weak. They do exist however and are quite accessible to $NH_3$ adsorption. These sites may offer catalytic usefulness for reactions requiring weak, nondestructive cationic sites or acid-base sites.

Carbon Dioxide Adsorption

When $CO_2$ was adsorbed onto $La_2O_3$ at 50°C the most intense bands are observed instantly at 1492 and 1389 $cm^{-1}$. They reach their maximum intensity within 5-10 minutes, the final intensity being independent of the $CO_2$ pressure. A sequence of spectra appear in Figure 2 and depict $CO_2$ adsorption onto $La_2O_3$ at 50°C followed by vacuum heating of chemisorbed species. Broad bands are observed at 1492 and 1389 $cm^{-1}$. Vacuum heating at 350°C generates two less intense bands which appear at 1568 and 1306 $cm^{-1}$. Chemisorption of excess $CO_2$ at 350°C does not result in significantly increased band intensities at 1568 and 1306 $cm^{-1}$. The concentration of the adsorbed species is limited by the number of adsorption sites. The bands at 1492 and 1389 $cm^{-1}$ are due to the antisymmetric stretching mode of a unidentate carbonate species formed from the reaction of gas phase $CO_2$ with surface $O^{-2}$ ions. Much less intense bands were also observed at 1060 and 850 $cm^{-1}$ which can be assigned to the symmetric stretching and deformation vibrational modes of the same species, respectively.

The $CO_2$ adsorption experiments were repeated using C-13 and O-18 isotopically labeled $CO_2$ gasses. With C-13 labeling the band due to the

antisymmetric stretch at 1492/1389 $cm^{-1}$ shifts to 1452/1378 $cm^{-1}$, and it shifts to 1477/1378 $cm^{-1}$ for O-18 labeling. Therefore, observed for C-13 labeling was a shift of 40 and 11 $cm^{-1}$, and for O-18 labeling, a shift of 15 and 11 $cm^{-1}$, for the antisymmetric and symmetric stretching components, respectively. These shifts are consistent with those expected from the assigned species (11). The following mechanism applies.

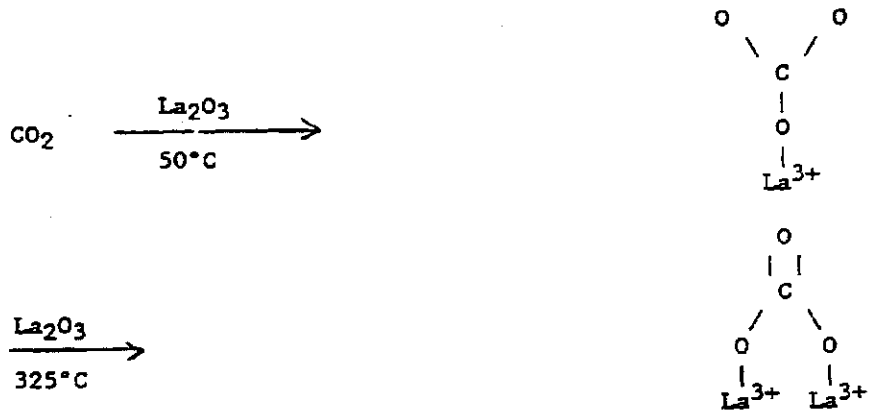


Many investigators have examined $CO_2$ adsorption onto metal oxides. Hair has summarized the possible modes of $CO_2$ adsorption onto basic oxides and has reviewed IR adsorption studies (5). Rosynek and Magnuson reported $CO_2$ adsorption followed by vacuum heating on $La_2O_3$ (12). The present investigation reports similar results. Rosynek et al. quantified the $CO_2$ adsorption using a microbalance and determined that the surface coverage was about 7-8 $CO_2$ molecules/100 $A^2$. For hexagonal $La_2O_3$ this value corresponds to approximately one $CO_2$ molecule per surface $O^{-2}$ ion, resulting in complete coverage of the surface oxides. A study of $CO_2$ adsorption on $Sc_2O_3$ at 250°C reported similar results. Evidence was found indicating symmetric carbonate species, which displayed a single band at 1330 $cm^{-1}$, and also bidentate carbonate species, which displayed bands at 1440 and 1220 $cm^{-1}$ (13). On

alumina, more weakly held surface carbonates were formed by the reaction of $CO_2$ with surface oxides (14). Bicarbonate species were also observed following lower pretreatment tempertures. The IR spectrum of a few lanthanide carbonates was published by Caro, Sawyer and Eyring including a spectrum of $La(CO_3)_3 \cdot 8H_2O$ (15). This spectrum of this compound is very similar to that of the $La(OH)_3$ starting materials used in the present study. Caro et al. prepared the carbonates by stirring powdered oxides in water using CO gas. It took 24 hours to convert the oxides. A somewhat similar reaction occurs when the hydroxide starting materials are slowly contaminated by gas phase $CO_2$ in a humid atmosphere. They observed bands at 1460, 1360, 1075, and 850 $cm^{-1}$, and concluded that the $CO_3^{-2}$ group in the rare earth normal carbonate exhibits the IR spectrum of a unidentate coordinated carbonate ion. On nickel oxide, $CO_2$ adsorption resulted in bands at 1620 and 1360 $cm^{-1}$. These bands were attributed to either bicarbonate or bidentate coordination (16). This behavior is very unlike that on $La_2O_3$.

$NH_3$ and $CO_2$ Coadsorption

An interesting surface reaction between $NH_3$ and $CO_2$ was observed to occur on $La_2O_3$. Shown in Figure 3 is the result of reacting an equimolar $NH_3$ and $CO_2$ gas mixture over $La_2O_3$ at 50°C. Surface species immediately developed as was evidenced by the appearance of three bands at 1622, 1533, and 1449 $cm^{-1}$. No other bands were discernible. In Figure 4 changes in the band's intensities are shown following vacuum heating of these surface species. Vacuum heating at only 200°C caused the three bands to vanish simultaneously, while at the same time a new band at 2171 $cm^{-1}$ developed. With higher temperature vacuum heating this band was slowly replaced by a band at 1985 $cm^{-1}$. Therefore, three independent species are responsible for

this series of bands. Heating at higher temperatures for longer periods eventually caused removal of the 1985 $cm^{-1}$ band, with a concomittant generation of a broad, featureless band in the 1700-1250 region, due to the CN stretch of heterogeneous, poorly-defined, polymeric materials.

When the chemisorbed forms of $NH_3$ and $CO_2$ were reacted by sequential adsorption and evacuation of each gas, the above reaction only occured if the order of adsorption and evacuation at 50°C was $NH_3$ and then $CO_2$. The reaction is therefore between chemisorbed $NH_3$ and gas phase $CO_2$. The unidentate carbonate species did not react with either gas phase or chemisorbed $NH_3$. As described above, the same bonds can also be generated, to a slightly greater maximum intensity, by adsorbing a gas mixture of $NH_3$ and $CO_2$ at the same temperature required for the conversion of the chemisorbed species. The adsorption sites for $NH_3$ and $CO_2$ on $La_2O_3$ therefore behave independently.

Isotopically labeled $NH_3$ and $CO_2$ gas combinations were also adsorbed at 50°C and the shifts observed for the bands at 1622, 1533, and 1449 $cm^{-1}$ were measured. For the 1622 $cm^{-1}$ band, a shift of 158 $cm^{-1}$ occurs for trideuterium labeling of the $NH_3$. This suggests a vibration involving a proton. Less significant shifts resulted for N-15 and C-13 labeling of 8 and 9 $cm^{-1}$, respectively; however, use of O-18 labeled $CH_2$ caused no shift at all. Based on these shifts and the band position, the origin of the vibration is an antisymmetric NH bending vibration of an amide species. For the 1533 $cm^{-1}$ band, significant shifts occured for C-13 and O-18 of 32 and 5 $cm^{-1}$, respectively, but insignificant shifts were observed for N-15 and trideuterium labeling. Similarly, for the 1449 $cm^{-1}$ band, significant shifts developed for C-13 and O-18 of 39 and 17 $cm^{-1}$, respectively. However, a

shift of 6 $cm^{-1}$ vibrations originate from the antisymmetric and symmetric stretch, respectively, of a carboxyl group. The wavenumber separation between the bands, as well as the band position of the antisymmetric stretch, normally increase with increasing oxygen coordination for carboxylic groups (2). Hence, these results indicate the formation of a surface carbamate species coordinated through an oxygen atom with the surface.

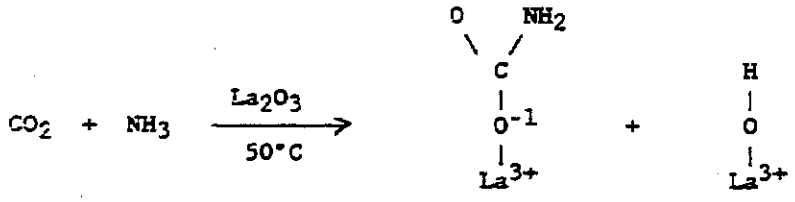


Such a species would generate three easily observed bands, viz., an antisymmetric and symmetric COO stretch and an $NH_2$ bending mode. The isotopic shifts they would display are within the correct magnitudes to match those observed (4,5). In addition, when an equimolar mixture of $NH_3$ and $CO_2$ is increased in pressure to about 100 torr, a white precipitate of ammonium carbamate forms. Ammonium carbamate actually originates from the reaction of unstable carbamic acid with excess $NH_3$. The reaction on the surface does not go far enough to produce ammonium carbamate since a much stronger base than the $NH_3$, the surface oxides themselves, compete successfully for the proton. Additionally, this is supported by the absence of a band due to $NH_2^+$ species in the 145 $cm^{-1}$ region. A noncatalytic industrial synthesis of urea by reacting $NH_3$ and $CO_2$ under heat and pressure was once developed in 1873 by Divers (17). The intermediate is ammonium carbamate which isomerized to urea (18). In fact, urea is still produced by a similar process today (19). Francis and Thorne reported using organo-tin catalysts to prepare a large

number of new carbamates of tertiary alcohols which can be used in new synthetic routes (20).

The isotopic labeling results for the 2171 $cm^{-1}$ band are depicted in Table 1. They are also compared to the band position and isotopic shifts for ionic cyanate ions dissolved in solid solution (21,22). The isotopic shifts as well as the band positions agree closely. Cyanate ions on $La_2O_3$ would form an ionic bond. The N-15 shift of 17 $cm^{-1}$ is characteristic of cyanates; no other simple carbon, nitrogen, or oxygen compounds would be expected to show this small a shift. For example, ionic cyanides typically show an N-15 of 34 $cm^{-1}$, and that expected for fulminates is 37 $cm^{-1}$ (11). The cyanide stretching region has received much attention for organic and transition metal inorganic cyanides (23, 24, 25) and even for the lanthanide and actinide cyanides (26). Because of their size, the lanthanides tend to accommodate a number of cyanide ligands easily, and IR spectra typically reveal more than one band in the 2180-2080 $cm^{-1}$ region. Although 2171 $cm^{-1}$ would be high for the La-CN stretch, cyanides cannot be ruled out by the position of the band alone. The isotopic shift data, however, definitely rules out cyanide species and suggests the generation of cyanate ions from $NH_3$ and $CO_2$ exposure. This reaction appears to have been previously unreported. Generating cyanates from $NH_3$ and $CO_2$ would be expected to occur in the presence of a strong dehydrating agent, in this case the surface $O^{-2}$ ions (18,27,28,29). The balanced overall eqution for this process is: $NH_3 + CO_2 \quad HOCN + H_2O$. The HOCN remains adsorbed on the surface as cyanate and hydroxyl ions.

The shifts observed for the 1981 $cm^{-1}$ band are very similar to those observed for the 2171 $cm^{-1}$ band. For both these bands, N-15 and C-13

labeling results in shifts of about 18 and 54 $cm^{-1}$, respectively, and a shift of about 5 $cm^{-1}$ for O-18 labeling. Deuterium labeling results in no shift. The specific origin of these shifts is uncertain but their similarity to the shifts observed for the 2171 $cm^{-1}$ band indicate that only a slight alteration of structure could have occurred. A slight change in the way to cyanate is bound to the surface could cause such an observation.

A few adsorption studies of isocyanate stability on metal oxides have appeared. On acidic oxides, covalently bonded isocyanates with nitrogen coordination would predominate over true cyanates, which are usually unstable (2). Solymosi et al. have reacted NO and CO over oxide-supported platinum catalysts at 250°C to generate surface isocyanates (30). IR bands believed to belong to adsorbed cyanates were observed at 2272, 2318, 2241 and 2210 $cm^{-1}$ for $Al_2O_3$, $SiO_2$, MgO, and $TiO_2$, respectively. Bands were absent when NO and CO were reacted on the supports themselves; however, there is evidence that isocyanates form on the metal and then transfer to the support (31). The CN triple-bond stretching node shifts to lower frequency with greater electron withdrawal from the CN triple bond. On $Cr_2O_3$ the NO and CO reaction has received a good deal of attention because it has been assumed that isocyanate surface species may play a role in the undesirable formation of $NH_3$ and HCN during the catalytic treatment of automobile exhaust gasses (31). On $Cr_2O_3$, a band at 2150 $cm^{-1}$ was assigned to a Cr-CN species and a band at 2210 $cm^{-1}$ was assigned to a nitrogen coordinated NCO species coordinated to a chromium ion. By adsorbing isocyanic acid, HNCO, at 298 K, the same bands were generated. Cyanates adsorbed onto basic $La_2O_3$ would be bound ionically with the degree of oxygen coordination quite small. This would result in low frequencies for the CN stretch.

HCN Adsorption

The result of adsorbing HCN is shown in Figure 5. Essentially identical bands develop in the case of HCN adsorption, as was observed with $NH_3$ and $CO_2$ coadsorption. However, when HCN is adsorbed, the bands each develop at lower temperatures. This explains the slight shift to lower wavenumbers illustrated by the band at 2164 $cm^{-1}$. With adsorption at 50°C, less energetic sites were coordinated than if the adsorption was performed at 250°C. The reaction is slow, taking almost two hours for the 2164 $cm^{-1}$ band to reach its maximum intensity at 50°C. HCN is a very weak acid. On the other hand, $CN^-$ ions are extremely strong bases, and perhaps while they are on the surface, they are even stronger bases than $O^-_2$ or $OH^-$ ions. The initial step in this reaction is certainly the removal of a proton from the HCN molecule. The next step is uncertain. Because of the presence of an electron accepting site, the liberated cyanides are oxidized to cyanates. The source of these electron accepting sites may involve minute quantities of adsorbed oxygen, either introduced with the adsorbate or collected from vacuum. Another explanation could be an induced surface reduction, under these extreme conditions, of $La^{3+}$ to $La^{1+}$ ions. Oxidation of cyanides to cyanates is not difficult. The introduction of cyanide into molten KBr produces mostly cyanate by atmospheric oxidation (22). The mechanism below describes this observation.

The reaction of HCN or similar probe molecules on oxide surfaces has received some attention in recent years. Low et al. (32) and then Morrow and Cody (33) examined HCN and cyanogen, $C_2N_2$, adsorption onto silica at 800°C. They observed a number of bands in the 2300-2100 $cm^{-1}$ region. Some of the bands can definitely be assigned to nitrogen coordinated cyanate species.

This cyanide oxidation on silica is very similar to the present results for adsorption onto $La_2O_3$, except that on $La_2O_3$, following HCN adsorption at 50°C, only cyanate species were observed. The IR spectrum of adsorbed and polymerized HCN on 50°C vycor glass has been published. When the adsorbed HCN molecules polymerized, new bands were observed in the CN triple and double bond stretching regions (4,32).

Additional Adsorption Studies

Additional experiments further characterized the observed band-shift from 2171-1985 $cm^{-1}$ when the cyanate species were vacuum heated above 500°C. When an equimolar mixture of $NH_3$ and $CO_2$ was exposed at 336°C to the species which exhibited a band at 1985 $cm^{-1}$, the intensity of the 1985 $cm^{-1}$ band decreased, while that of the 2171 $cm^{-1}$ band increased. Therefore, the two species responsible for these bands can coexist on the surface. The decrease in the concentration of the more thermally stable species by $NH_3$ and $CO_2$ exposure represents an induced reversal of the equilibrium between the 2171 and 1985 $cm^{-1}$ species. In an attempt to reproduce this behavior using $CO_2$ alone, the experimental results illustrated in Figure 6 were obtained. Again, the 1985 $cm^{-1}$ band decreases, and the 2171 $cm^{-1}$ increases in intensity, as the concentration of surface unidentate carbonate species increases. To ensure that the $CO_2$ used in this experiment was $NH_3$ free, the $CO_2$ was first tested by exposing an excess amount of $CO_2$ to a clean $La_2O_3$ surface which was maintained at 280°C, followed by ensemble averaging of IR spectra over the cyanate region. No cyanate production meant no $NH_3$ impurity. The 1985 $cm^{-1}$ species must therefore arise from a change in the way the cyanate bonds to the surface, a change which can be reversed by the

adsorption of unidentate carbonate. A nondestructive reaction at that temperature which explains these observations appears below.

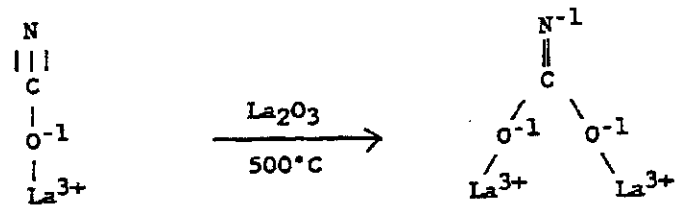


The cyanate was further oxidized by the surface from unidentate to bidentate coordination, much like the transition observed for $CO_2$ at this temperature. This would explain the very similar isotopic shifts observed for the 2171 and 1985 $cm^{-1}$ band.

These cyanate species were also reacted with water and oxygen at elevated temperatures. At 50°C, water has no effect within 30 minutes, but when left in the cell and then heated to 350°C for 20 minutes, both bands were completely removed. However, new bands also developed, and these are illustrated in Figure 7. Also included in this figure is the effect of vacuum heating on these new species. The result is identical to that obtained when a water and $CO_2$ mixture were exposed to $La_2O_3$ at 350°C. These new bands were produced when the surface cyanates were decomposed with water back to $CO_2$ and $NH_3$. The bands at 1507 and 1402 $cm^{-1}$ are due to unidentate coordinated carbonate. The band at 1339 $cm^{-1}$ is also due to carbonate, but ionically or symmetrically bound. Ionic carbonate species have been observed on other highly electropositive metal oxides (4). Similarly, $O_2$ treatment was investigated and was found to have no effect even when left in the cell

and heated to 336°C for 10 minutes; however, after about 30 minutes at 336°C, both bands vanished. The 1985 $cm^{-1}$ band decreased first, but both bands gradually decreased and no new bands developed.

## CONCLUSION

Chemisorbing $NH_3$ onto $La_2O_3$ at 50°C led to only one transmission IR band appearing at 1092 $cm^{-1}$ in the presence of gas phase $NH_3$. The band shifted to 1135 $cm^{-1}$ following $NH_3$ evacuation. The band vanished following vacuum heating at 130°C. The vibration originated from the symmetric stretching mode of an $NH_3$ molecule coordinately bound to an exposed $La^{3+}$ site. On the other hand, adsorbing $CO_2$ onto $La_2O_3$ at 50°C yielded bands characteristic of a unidentate carbonate, which following vacuum heating at 350°C was converted to bidentate coordination. By reacting a mixture of the gasses, a number of distinct surface species were generated depending upon the temperature of exposure. At 50°C, surface carbamate ions were formed, while at 200°C, cyanate ions undergo a transition from unidentate to bidentate coordination at about 500°C similar to that observed for the carbonate ions. Isotopically-labeled $NH_3$ and $CO_2$ were used to verify these assignments.

The synthesis of cyanate species from $NH_3$ and $CO_2$ is an unusual one. Although urea is synthesized industrially from the reaction of $NH_3$ and $CO_2$, further dehydration to produce cyanate is an unusual reaction, characteristic of the extremely dehydrating nature of $La_2O_3$ (19). Because of the importance of cyanide and cyanate polymeric materials, the use of $NH_3$ and $CO_2$ or similarly reacting amines and carboxylates to generate cyanate containing entities may be significant.

## REFERENCES


(1) Yu. S. Khodakov, V.V. Lobachev, and Kh. M. Minachev, Izvestiya Akademii Nauk SSSR, Seriya Khimicheskaya, 10, 2167 (1975).

(2) N. Nakamoto, "Infrared Spectra of Inorganic and Coordination Compounds." John Wiley and Sons, N.Y., 1970.

(3) G.F. Svatos, D.M. Sweeny, S. Mizushima, C. Curran, and J.V. Quagliano, J. Amer. Chem. Soc. 79, 3313 (1957).

(4) L.H. Little, "Infrared Spectra of Adsorbed Species." Academic Press, N.Y., 1966.

(5) M.L. Hair, "Infrared Spectroscopy in Surface Chemistry." Marcel Dekker, Inc., N.Y., 1967.

(6) A.V. Kiselev and V.I. Lygin, "Infrared Spectra of Surface Compounds." John Wiley and Sons, N.Y., 1975.

(7) J.B. Peri, J. Phys. Chem. 69, 231 (1965).

(8) A.A. Tsyganenko, D.V. Pozdnyakov, and V.N. Filimonov, J. Molecular Structure 29, 299 (1975).

(9) T. Morimoto, H. Yana, and M. Nagao, J. Phys. Chem. 80, 471 (1976).

(10) T. Moeller, "The Chemistry of the Lanthanides." Pergamon, N.Y., 1975.

(11) S. Pinchas and I. Laulicht, "Infrared Spectra of Labeled Compounds." Academic Press, N.Y., 1971.

(12) M.P. Rosynek and D.T. Magnuson, J. Catal. 48, 417 (1977).

(13) J.A. Pajares, J.E. Gonzalez de Prado, J.L. Garcia Fierro, L.G. Tejuca, and S.W. Weller, J. Catal. 44, 421 (1976).

(14) M.P. Rosynek, J. Phys. Chem. 79, 1280 (1975).

(15) P.E. Caro, J.O. Sawyer, and L. Eyring, Soectrochim. Acta 28A, 1167 (1972).

(16) M. Courtois and S.J. Teichner, J. Catal. 1, 121 (1962).

(17) E. Divers, Trans. Roy. Soc. (London) 163, 372 (1873).

(18) A.F. Hegarty, in "Comprehensive Organic Chemistry, Vol. 2, Nitrogen Compounds, Carboxylic Acids, Phosphorous Compounds." (I>C. Sutherland, ed., p. _067, Pergamon Press, N.Y., 1979.

(19) M. Heylin, ed., Chem. Eng. News 60, 22 (1982).

(20) T. Francis and Mr. Thorne, Can. J. Chem. 54, 24 (1976).

(21) D.F. Smith, J. Overend, J.C. Decius, and D.J. Gordon, J.Phys. Chem. 58, 1636 (1973).

(22) A. Maki and J.C. Decius, J. Chem. Phys. 31, 772 (1959).

(23) M.F. Amr El sayed and R.K. Sheline, J. Inorg. Nucl. Chem. 6, 187 (1958).

(24) L.H. Jones, Inorg. Chem. 2, 777 (1963).

(25) J.R. Ferraro, "Low-Frequency Vibrations of Inorganic and Coordination Compounds." Plenum Press, N.Y., 1971.

(26) I.J. McColm and S. Thompson, J. Inorg. Nucl. Chem. 34, 3801 (1972).

(27) E.E. Royals, "Advanced Organic Chemistry." Prentice-Hall, N.Y., 1954.

(28) J.D. Roberts and M.C. Caserio, "Basic Principles of Organic Chemistry." W.A. Benjamin, Inc., N.Y., 1965.

(29) R.T. Morrison and R.N. Boyd, "Organic Chemistry." Allyn and Bacon, Boston, 1973.

(30) F. Solymosi, K. Volgyesi, and J. Sarkany, J. Catal. 54, 336 (1978).

(31) F. Solymosi and T. Bangagl, J. Phys. Chem. 83, 552 (1979).

(32) M.J.D. Low, N. Ramasubramanian, P. Ramamurthy, and A.V. Deo, J. Phys. Chem. 72. 2371 (1968).

(33) B.A. Morrow and I.A. Cody, J. Chem. Soc. Faraday Trans.-1 71, 1021 (1975).

TABLE 1

| Isotopic Labelling Results for $NH_3 + CO_2$ Co-adsorption on $La_2O_3$ for the 2171 $cm^{-1}$ Band | | Obs. C≡N Stretching Freqs. for Isotopically Labelled $NCO^-$ in Ionic Salts | |
|---|---|---|---|
| Isotopic Labelling | Isotopic Shift ($cm^{-1}$) | Isotopic Labelling | Isotopic Shift ($cm^{-1}$) |
| $^{14}NH_3/^{12}C^{16}O_2$ | — | $^{14}N\equiv^{12}C-^{16}O^-$ | — |
| $ND_3$ | -1 | — | — |
| $^{15}N$ | -17 | $^{15}N$ | -18 |
| $^{13}C$ | -59 | $^{13}C$ | -57 |
| $^{18}O$ | -6 | $^{18}O$ | -8 |

FIGURE CAPTIONS

Fig. 1 $NH_3$ adsorption onto $La_2O_3$ at 50°C. Spectrum (a) is the $La_2O_3$ background. Following exposure to 5 torr of $NH_3$ at 50°C, spectrum (b) was obtained, and after evacuation for 10 minutes at 50°C, spectrum (c) was taken . Difference spectra appear in (d) and (e) as indicated.

Fig. 2 $CO_2$ adsorption onto $La_2O_3$ at 50°C followed by vacuum heating. In spectrum (a), 128 torr of CO(2) were exposed for 10 minutes followed by 10 minutes of evacuation at 50°C. Vacuum heating for 15 minutes at each of the indicated temperatures resulted in spectra (b)-(d).

Fig. 3 Sequential exposure of $NH_3$ and $CO_2$ to $La_2O_3$ at 50°C. Spectrum (a) results from exposing 98 torr of $CO_2$ for 10 minutes, followed by 10 minutes of evacuation at 50°C. Following removal of these bands by oxygen and vacuum treatment at 800°C, in spectrum (b) 100 torr of $NH_3$ were exposed to the sample at 50°C for 7 minutes, followed by 10 minutes of evacuation at 50°C. Then, in spectrum (c), 103 torr of $CO_2$ were exposed for 10 minutes, followed by 10 minutes of evacuation at 50°C. Spectrum (d) is the result of subtracting spectrum (a) from spectrum (c).

Fig. 4 Result of vacuum heating on the bands generated by sequential exposure of $NH_3$ and $CO_2$ to $La_2O_3$ at 50°C. First, 100 torr of $NH_3$ were exposed for 7 minutes, followed by 10 minutes of evacuation at 50°C. Next, 103 torr of $CO_2$ were exposed to the sample for 10 minutes at 50°C, followed by 10 minutes of evacuation at 50°C. These spectra were obtained following 15 minutes of vacuum treatment at each of the indicated temperatures.

Fig. 5 HCN adsorption onto $La_2O_3$ at 50°C followed by vacuum heating. After exposing 2 torr of HCN for 5 minutes at 50°C, spectrum (a) was taken. Spectrum (b) resulted following evacuation for 15 minutes. Subsequent vacuum heating of this species for 15 minutes at each temperature indicated resulted in spectra (c)-(f).

Fig. 6 Effect of $CO_2$ adsorption at 336 and 50°C on the bands resulting from the reaction of $NH_3$ and $CO_2$ on $La_2O_3$ at 410°C. In spectrum (a), 20 torr of an equimolar mixture of $NH_3$ and $CO_2$ were exposed at 410°C for 15 minutes, followed by 10 minutes of evacuation at 410°C and 20 minutes at 350°C. In spectrum (b), 11 torr of $CO_2$ were then exposed to the sample at 336°C for 20 minutes, followed by 5 minutes of evacuation at 336°C. After additional exposure to 10 torr of $CO_2$ at 50°C for 15 minutes and evacuation for 10 minutes at 50°C, spectrum (c) was taken.

Fig. 7 Effect of vacuum heating on the bands generated by $H_2O$ exposure at 350°C to $La_2O_3$ which had been previously exposed to an equimolar mixture of $NH_3$ and $CO_2$ at 320°C. First, 20 torr of an equimolar mixture of $NH_3$ and $CO_2$ were exposed at 320°C for 10 minutes, followed by 10 minutes of evacuation at 320°C. Next, 20 torr of $H_2O$ were added to the cell, and kept in the cell while the sample was heated to 350°C for 20 minutes, followed by evacuation at 350°C for 10 minutes. Finally, to obtain spectra (a)-(c), the resulting species was vacuum heated at each of the indicated temperatures for 25 minutes.

FIG. 1

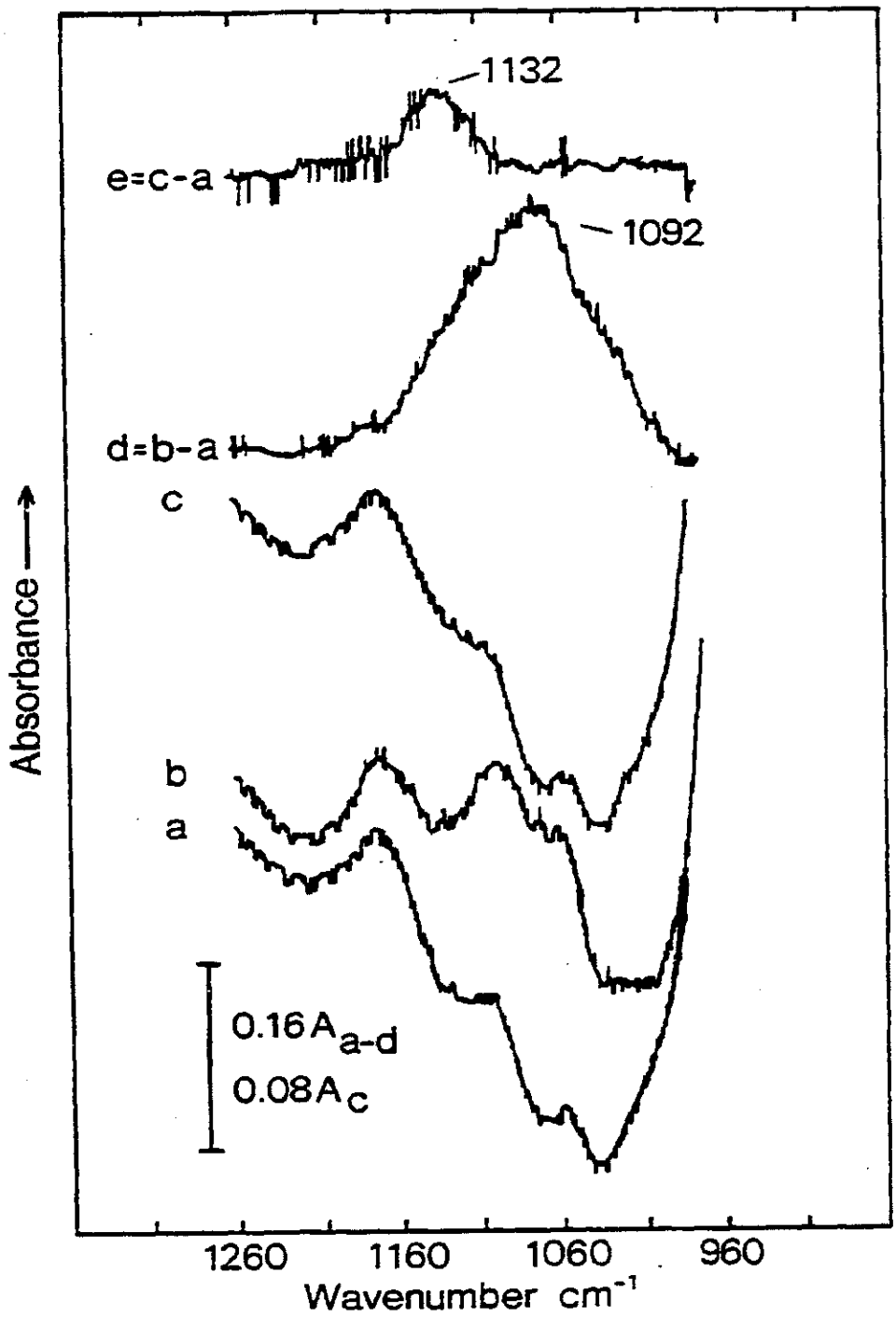
1132
e=c-a
1092
d=b-a
c
b
a
Absorbance
0.16 A a-d
0.08 A c
1260
1160
1060
960
Wavenumber cm-1

FIG. 2

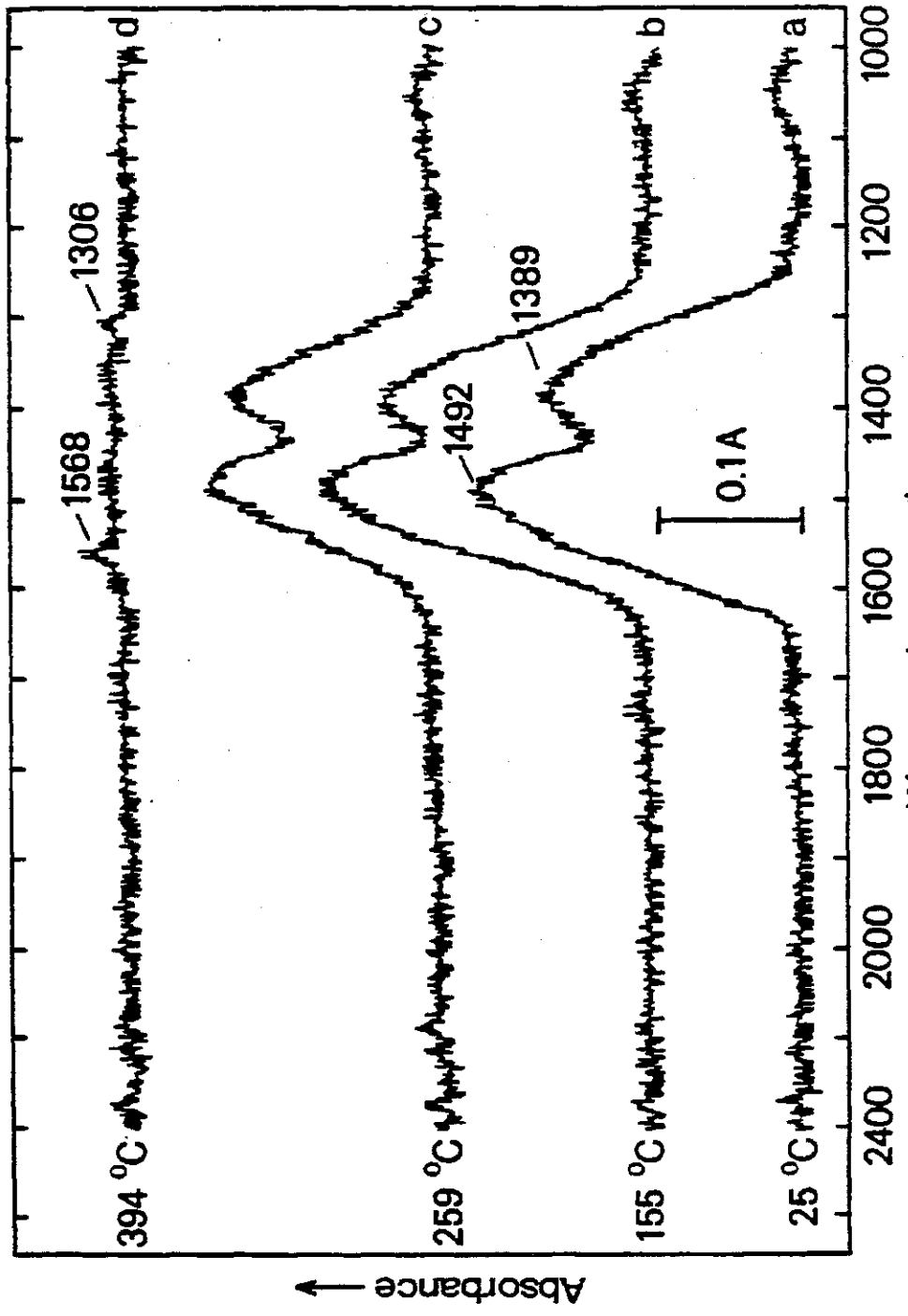
394 °C
259 °C
155 °C
25 °C
d
c
b
a
1568
1306
1492
1389
0.1A
2400
2000
1800
1600
1400
1200
1000
Wavenumber, cm⁻¹
Absorbance

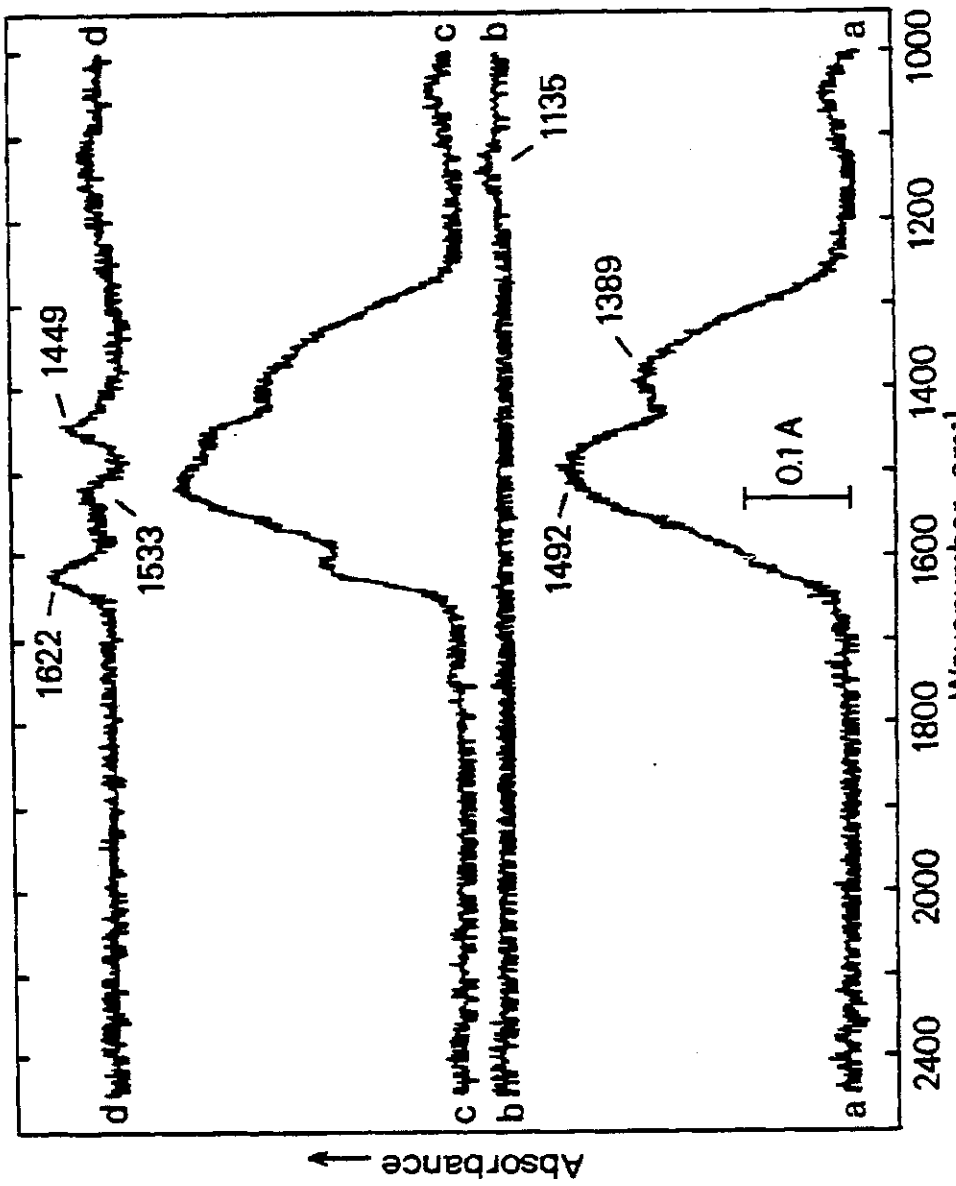
Absorbance
Wavenumber, cm-1
2400
2000
1800
1600
1400
1200
1000
1622
1533
1449
1492
1389
1135
0.1 A
a
b
c
d

FIG. 3

FIG. 4

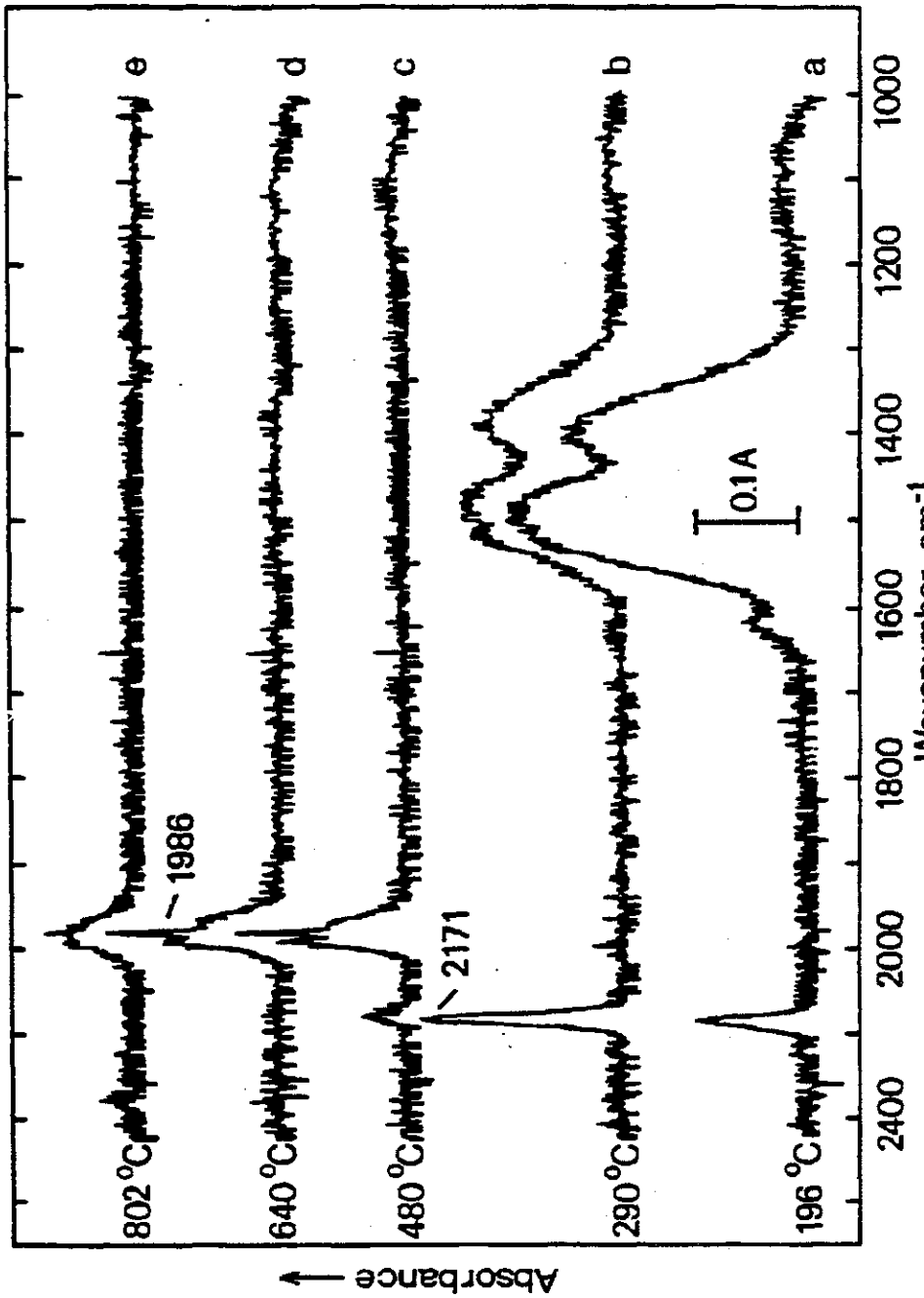
802 °C
640 °C
480 °C
290 °C
196 °C
e
d
c
b
a
1986
2171
0.1A
Absorbance
2400
2000
1800
1600
1400
1200
1000
Wavenumber, cm-1

FIG. 2

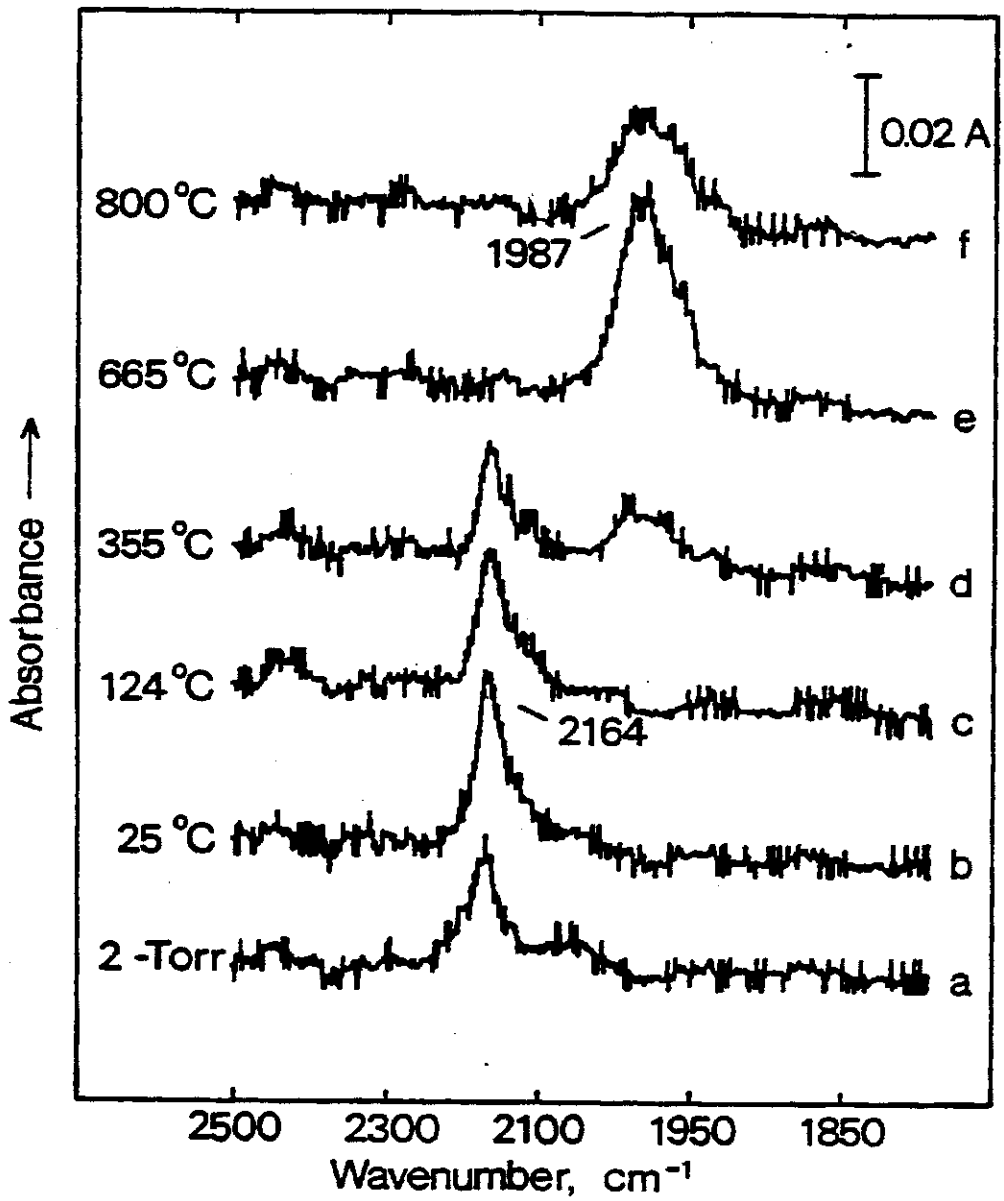
0.02 A
800 °C
1987
f
665 °C
e
355 °C
d
124 °C
2164
c
25 °C
b
2 -Torr
a
Absorbance
2500
2300
2100
1950
1850
Wavenumber, cm⁻¹

FIG. 6

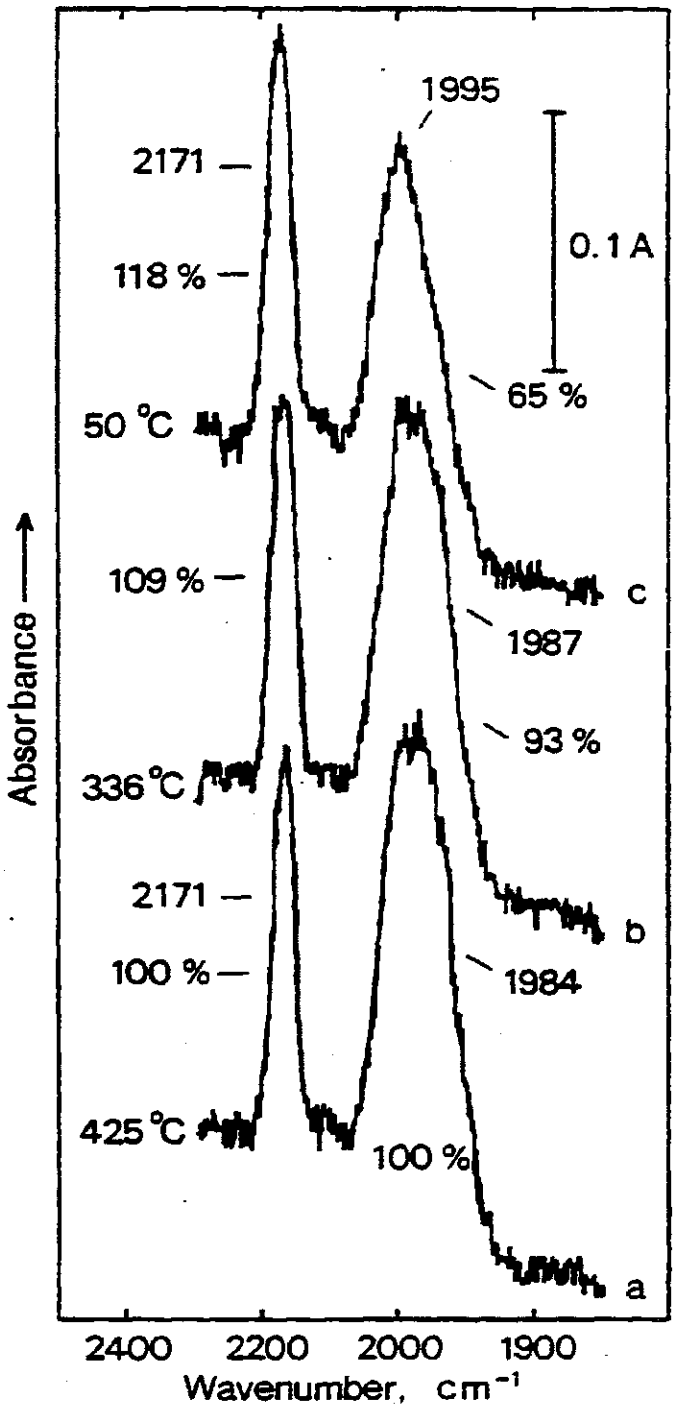
1995
2171
118 %
0.1 A
65 %
50 °C
c
109 %
1987
93 %
336 °C
2171
b
100 %
1984
425 °C
100 %
a
Absorbance
2400
2200
2000
1900
Wavenumber, cm⁻¹

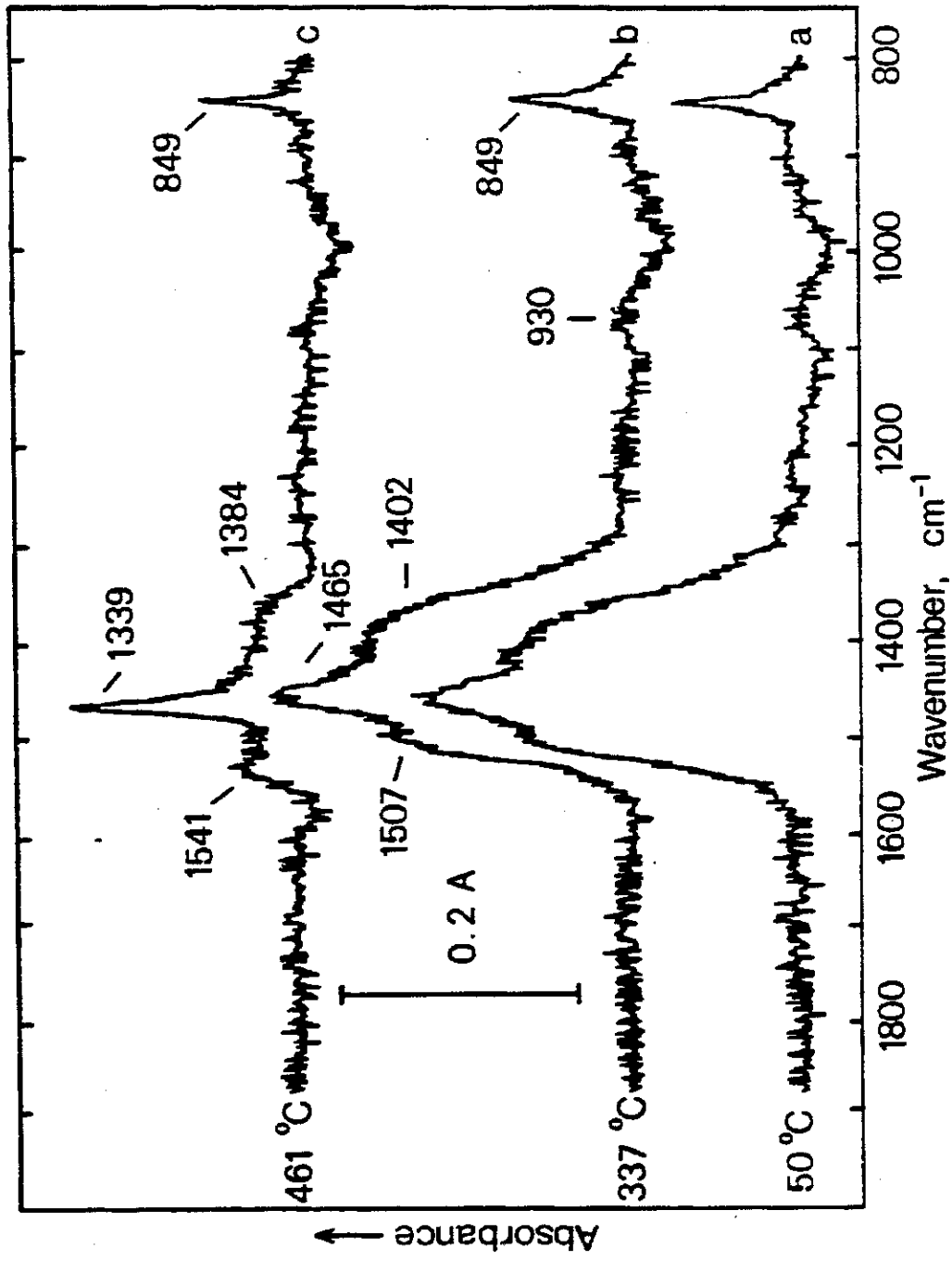
Absorbance
Wavenumber, cm$^{-1}$
1800
1600
1400
1200
1000
800
461 °C
337 °C
50 °C
a
b
c
0.2 A
1541
1507
1339
1465
1384
1402
930
849
849